(2)

NAVAL POSTGRADUATE SCHOOL
Monterey, California

THESIS

EFFECTS
OF THE NORTHEAST MONSOON ON
THE EQUATORIAL WESTERLIES OVER
INDONESIA

by

Chen, Chih-Lyeu

June 1990

Co-Advisor	M.S. Peng
Co-Advisor	C.-P. Chang

REPORT DOCUMENTATION PAGE

1a Report Security Classification: Unclassified			1b Restrictive Markings
2a Security Classification Authority			3 Distribution Availability of Report: Approved for public release: distribution is unlimited.
2b Declassification Downgrading Schedule			
4 Performing Organization Report Number(s)			5 Monitoring Organization Report Number(s)
6a Name of Performing Organization: Naval Postgraduate School	6b Office Symbol (if applicable): MR		7a Name of Monitoring Organization: Naval Postgraduate School
6c Address (city, state, and ZIP code): Monterey, CA 93943-5000			7b Address (city, state, and ZIP code): Monterey, CA 93943-5000
8a Name of Funding Sponsoring Organization	8b Office Symbol (if applicable)		9 Procurement Instrument Identification Number
8c Address (city, state, and ZIP code)			10 Source of Funding Numbers: Program Element No / Project No / Task No / Work Unit Accession No

11 Title (include security classification): EFFECTS OF THE NORTHEAST MONSOON ON THE EQUATORIAL WESTERLIES OVER INDONESIA

12 Personal Author(s): Chen, Chih-Lyeu

13a Type of Report	13b Time Covered	14 Date of Report (year, month, day)	15 Page Count
Master's Thesis	From To	June 1990	65

16 Supplementary Notation: The views expressed in this thesis are those of the author and do not reflect the official policy or position of the Department of Defense or the U.S. Government.

17 Cosati Codes			18 Subject Terms (continue on reverse if necessary and identify by block number)
Field	Group	Subgroup	winter monsoon surge, ITCZ, cross equatorial flow, XEF, WAT

19 Abstract (continue on reverse if necessary and identify by block number)

The possible cross equatorial influences of the Northern Hemisphere on the zonal wind along 10° S in the Indonesia-Arafura Sea region are studied by using a 14-year data set. Composites of time series of individual circulation parameters and surface flow charts reveal a correlation between the northeastern monsoon of the Northern Hemisphere and the Southern Hemisphere summer monsoon. The correlation is significantly stronger during the middle season compared to late season. During the late season distinct patterns of changes are found in the Australian monsoon trough and upper tropospheric flow. This reflects a stronger connection between summer monsoon and midlatitude baroclinic systems within the Southern Hemisphere. Thus the mid-season events of the southern monsoon wind strengthening are more influenced by surges in the northeast monsoon in the Northern Hemisphere; while the late-season events may be due to midlatitude baroclinic effects in the Southern Hemisphere rather than the northern cold surges.

20 Distribution Availability of Abstract	21 Abstract Security Classification	
☒ unclassified unlimited ☐ same as report ☐ DTIC users	Unclassified	
22a Name of Responsible Individual: M.S. Peng	22b Telephone (include Area code): (408) 646-2722	22c Office Symbol: MR PG

DD FORM 1473,84 MAR — 83 APR edition may be used until exhausted. All other editions are obsolete — security classification of this page

Approved for public release; distribution is unlimited.

Effects
of the Northeast Monsoon on
the Equatorial Westerlies over Indonesia

by

Chen, Chih-Lyeu
Lieutenant Commander, R.O.C Taiwan Navy
B.S., Taiwan Provincial College of Marine and Oceanic Technology

Submitted in partial fulfillment of the
requirements for the degree of

MASTER OF SCIENCE IN METEOROLOGY AND OCEANOGRAPHY

from the

NAVAL POSTGRADUATE SCHOOL
June 1990

Author: Chen, Chih-Lyeu

Chen, Chih-Lyeu

Approved by: Melinda S. Peng

M.S. Peng, Co-Advisor

C.-P. Chang

C.-P. Chang, Co-Advisor

Robert J. Renard

Robert J. Renard, Chairman,
Department of Meteorology

ABSTRACT

The possible cross equatorial influences of the Northern Hemisphere on the zonal wind along 10° S in the Indonesia-Arafura Sea region are studied by using a 14-year data set. Composites of time series of individual circulation parameters and surface flow charts reveal a correlation between the northeastern monsoon of the Northern Hemisphere and the Southern Hemisphere summer monsoon. The correlation is significantly stronger during the middle season compared to late season. During the late season distinct patterns of changes are found in the Australian monsoon trough and upper tropospheric flow. This reflects a stronger connection between summer monsoon and midlatitude baroclinic systems within the Southern Hemisphere. Thus the mid-season events of the southern monsoon wind strengthening are more influenced by surges in the northeast monsoon in the Northern Hemisphere, while the late-season events may be due to midlatitude baroclinic effects in the Southern Hemisphere rather than the northern cold surges.

TABLE OF CONTENTS

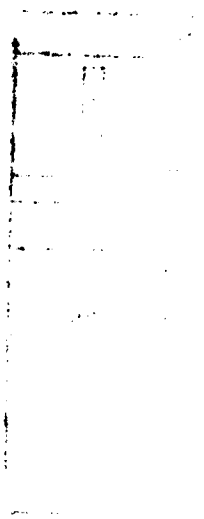

LIST OF TABLES

LIST OF FIGURES

ACKNOWLEDGEMENTS

I am particularily grateful to Professors Peng and Chang for their guidance, support and encouragement in this work.

I am most grateful to my wife, Chia-Huey, for her moral support and encouragement throughout my two years at the Naval Postgraduate School.

I. INTRODUCTION

The importance of the monsoons in the North Hemisphere, as one of the most energetic heat engines in driving the earth's atmosphere, has attracted a large number of tropical meteorologists. While, on the contrary, the monsoons of the South Hemisphere have received much less attention except by scientists in the region directly influenced by them. One main reason for scientists to neglect the South Hemisphere summer monsoon subject is due to lack of data over the South Hemisphere summer monsoon region until the 1970's (Murakami and Sumi 1982a).

As a consequence of the Monsoon Experiment (Winter Monex) during 1978-1979, which is designed to study several important questions of the winter monsoon, many new findings on the monsoon are revealed. Besides Monex, southern oscillation phenomena, known as EL Niño, have for many years drawn many researchers to investigate the relationships between the Southern Hemisphere monsoon and the southern oscillation. Holland and Nicholls (1985) have shown that EL Niño coincides with an early onset of the Australian monsoon in the preceding year, nearly 12 months earlier. Hereupon, there has been renewed interest in the world meteorological community on the Southern Hemisphere summer monsoon.

The first detailed studies of the time variations and three dimensional structure of summer circulation over northern Australia were performed by Troup and Berson (Berson 1961; Troup 1961; Berson and Troup 1961). Their studies demonstrate that the strength of the low-level monsoon westerlies is related to that of the upper-tropospheric easterly current (Troup 1961).

The equatorial trough (or intertropical convergence zone , ITCZ) is one of the most prominent features of the global atmospheric circulation in the tropics. Whenever the ITCZ is well removed from the equator, it is a zone of low pressure which separates Northern Hemispheric easterly trade wind flow on the northern side of it from the low-level westerly flow which is on the southern side of ITCZ. This type of ITCZ is referred to as "monsoon trough" (Gray 1968), and the westerly winds are called "monsoon westerlies". These monsoon westerlies will result in a high magnitude of rainfall along this zone of westerlies.

Broadly speaking, the summer monsoon of the Southern Hemisphere has many similarities with the northern summer monsoon over Southeast Asia and India. Bjerknes

(1969) and Krishnamurti et. al. (1973) showed the existence of strong east-west circulations in equatorial latitudes in addition to the Hadley-type circulations during Northern Hemisphere winter monsoon. The strongest of these circulations has rising motions over the maritime continents of Indonesia and Borneo, connected meridionally by sinking motions over Siberia and South Australia, and longitudinally by subsidence over the equatorial central Pacific and eastern Africa. Sumi and Murakami (1981) used a definition based on the low-level westerlies at 10° S. Applying this to the mean 850-mb wind field, they concluded that the Southern Hemisphere monsoon extended from the Indian Ocean (80°E) to the Central South Pacific (170°E). Furthermore, they concluded that the coupling of the upper-level easterlies / low-level westerlies characterizes the rotational wind component of the monsoon circulation, giving rise to a double Hadley cell structure over the monsoon longitudes. with the updraft center (ITCZ) lying along approximately 7° S. In addition , the latitudinal extent of the southern monsoon is more constrained than either the northern summer monsoon or the northern winter monsoon, extending poleward only along the Indonesian Islands, over Northern Australia and into the Solomon Sea with a large equatorward slope from the surface to the 850 mb level (Holland et.al. , 1984). The longitudinal extent is denoted by a band of strong westerlies along about 10° S from the northeastern Indian Ocean (100°E), across the Indonesian Seas and New Guinea, to the western South Pacific Ocean (180°E). The exact geographical extent is still unresolved yet. Furthermore, the southern summer monsoon also features active and break phases in monsoonal flow and convection. The suddeness of the change in the monsoon winds has been extensively investigated by Murakami and Sumi. et.al. (1982b). Inspection of their works indicates that a step - like change took place in the atmospheric circulation over the Southern Hemisphere monsoon region. The lower tropospheric westerlies and upper-level easterlies between the equator and 10° S can increase dramatically in strength. The events start when the Southern Hemisphere subtropical jet moves southward by more than 10° , followed by an intensification of the Northern Hemisphere subtropical jet several days later. The equatorial maximum cloud zone moves south by several degrees, and there is a large-scale increase in the extent and intensity of tropical convection. Also the geostationary meteorological satellite (GMS) cloud images reveal that the monsoon onset corresponds to a sudden transition from scattered random convection to spatially organized convection. Troup (1961) and Holland et al. (1984) indicate that the sudden increase in the monsoon winds is typical and that a sharp monsoon onset can be defined in most years.

As pointed out above, the zone of westerlies is typically one of high summer rainfall. Consequently, the definition of summer monsoon's onset is of interest to this study since an objective criterion of determining the onset is required in this context. The criterion used to describe monsoon onset are basically based on two categories: 1) enhanced activity in the winds , and 2) precipitation. Based on the observed rainfall at six stations within 300 km of Darwin (12° 26'S , 130°52'E), Troup noted a general association between rain events and westerly winds. The results of Troup's research show that the monsoon onset is related to a sudden increase in the upper-level easterly wind component at Darwin. Troup's (1961) rain criterion for monsoon onset based on daily observation at six stations close to Darwin, is defined as the first occasion after 1 November on which four or more stations record rainfall and the area-averaged rainfall over N days exceeds $0.75(N+1)$ inches for a time interval $(N+1)$ days. By his wind criteria, the onset date is the begining of the first spell of moderate west wind at the gradient level (3000 ft). A spell of moderate west wind which lasts for N days is defined as a period when the cumulative zonal components exceed 5.15 m s^{-1} for a time interval $(N+1)$ days, and the monsoon onset event is concluded when this component is less than 2.58m s^{-1} on two consecutive days. Besides the criteria for onset mentioned above, Davidson et.al. (1983) determined the onset date by analyzing satellite imagery and Holland et.al. (1984) objectively defined onset by using the direction, strength and constancy of the low-level wind field over northern Australia.

Despite the monsoon onset defined as either the first rain event or the first wind spell, the fact that no definition is universally accepted is due to marked regional differences in the behavior and timing of the onset over the region of the South Hemisphere's summer monsoon. However, it is worthwhile to note, Southern summer monsoon onset typically occurs between mid-December and mid-January. Many theories and hypotheses have been proposed to explain the triggering mechanisms for the onset of an action monsoon period in the Indonesia-Arafura Sea region. Some of the proposed mechamisms are described as follows.

- *Cold Surge in the South China Sea.* During the northern winter, the east Asia continent is dominated by a strong surface high over northern China and Siberia. A strong baroclinic zone exists between this cold, continental air mass and the warm tropical air mass to its south. As the pressure gradient across the East China tightens, cold air bursts out of the continent toward the South China Sea and a cold surge is initiated. Correspondingly, in the equatorial region, south of East Asia lies the maritime continent of Indonesia and Malaysia. During winter, extensive deep cumulus convection over this region supplies a large amount of latent heat to the atmosphere (Ramage 1971). From the results of a series of observa-

tional studies, Chang et al. (1979) and Chang and Lau (1980) noted that prior to the occurrence of a cold surge, the cooling due to advection over northern China strengthens the eastern Asia local Hadley cell. As a cold surge arrives at the equatorial South China Sea, the convection associated with pre-existing synoptic-scale disturbances flare up and warm the tropical atmosphere by release of latent heat. The upper-level outflow from the South China Sea convection region spreads mainly east and west, driving two Walker Circulation. Their main findings suggest that the winter monsoon cold surge is basically a phenomenon controlled by the northern midlatitude and its influences penetrate significantly eqatorward into tropics, and this equatorial convective heat source may interact with the cold surges, resulting in modifications of both synoptic and planetary scale motion. Through these complicated chains of midlatitude tropical and equatorial east-west interactions, the effect of an intense baroclinic development over the east Asia continent is spread deep across a wide equatorial belt ranging from East Africa to the mid-Pacific Ocean. Lim and Chang (1981) used linearized shallow water equations on an equatorial β plane to demonstrate the dynamic response of the tropical atmosphere to northern winter cold surges. Their studies were also supported by Davidson et al. (1983) who presented some data that suggested a possible relation between cold surges and the onset of the Australian monsoon. Williams (1981) also described a case of such cross-equatorial influence. He observed a slow pressure rise over Western Indonesia about three days after a surge crossed the South China Sea. In a composite of the surface flow patterns for the southern summers of 1974 to 1983, Shield (1985) used a 9-year data set and showed that the onset of the monsoon westerlies along 10^0 S in the Indonesian region is preceded by a significant strengthening of northeasterly monsoon winds that persist for three to four days. Once again, this result suggests that cold surges in the South China Sea may play an important role inbetween the midlatitude and tropics.

- *Southern Hemisphere's Tropical-Midlatitude Interactions.* Davidson et al. (1983) hypothesized that the onset of convection is strongly influenced by synoptic events in the Southern Hemisphere subtropics. Their observations shows that the subtropical ridge is interrupted over the southwestern corner of Australia by a trough, which extends westward into the low latitudes (approximately to 10^0 S). Besides affecting the continuity of the subtropical ridge, the trough also brings about a discontinuity in the monsoon shear line. Subsequently, during the following days the westerly trough drifts eastward and anticyclogenesis takes place over southwestern and south-central Australia. The anticyclogenesis persists until the sudden blowup of tropical convection occurs at onset. Thus, these observations show that the year-to-year similarity in the synoptic sequence constitutes evidence that the tropical convection is influenced by high- and low-pressure system movement and development in the Southern Hemisphere subtropics. Nevertheless, as hypothesized by Davidson et al. (1983), this subtropical synoptic sequence is not being proposed as the primary forcing mechanism for the onset of the monsoon. The primary forcing for monsoonal circulation is from differential heating of land and ocean regions due to seasonally changing solar radiation inputs (Webster 1981). Once the planetary scale temperature gradients have developed to a stage where the troposphere is in a state of readiness for the monsoon onset, thus, the point of all of this is, that the shorter-time-scale subtropical high-low pressure sequence becomes an important trigger (Davidson 1981). McBride (1983b) also shows that there are additional interactions between tropical convection and the midlatitude / subtropics of the Southern Hemisphere. By performing synoptic case studies of

41 tropical heavy-rain events, he found only 15% of the tropical systems had a link at the surface to a midlatitude westerly trough.

- *Surge of Low-Level Southerly Winds along the Western Australian Coast.* Davidson et al. (1983) observed that,prior to onset, a surge of low-level southerly winds parallels the western Australian coast. These surges have been linked physically to the intensity of Indian Ocean anticyclones and the passage of frontal systems past the southwest corner of the Australia. The intesity of the surge can be quantified in terms of the southerly component of geostrophic wind calculated at 20° S over the 100° - 120°E longitude band. Results from Davidson et al. (1983) research shows that a southerly geostrophic surge greater than 7.2 ms^{-1} was present within the five days preceding the onset. Thus, their significance in triggering monsoon convection may be an important component in the South Hemisphere midlatitude interaction with the tropics.

- *Westward Expansion of Monsoon Westerlies.* Using data collected during the Winter Monsoon Experiment (WMONEX) of December 1978 to February 1979, Murakami and Sumi (1982b) suggested that the monsoonal onset was initiated by events occurring away from the Indonesia-Arafura Sea region. Due to northeasterly trade wind intensification over the tropical North Pacific Ocean, cross equatorial northwesterlies result near 170° E. This induces a zone of strong westerlies which expand westward into the Indonesia-Arafura Sea region and establish the monsoon.

The purpose of this study is to extend Shield's (1985) study and investigate the possible influences of the northeast monsoon in the Northern Hemisphere on the south Hemisphere's summer monsoon, using a 14-year data set: 1974-1988 winter data. These data are the most recently available operationally analyzed data for the global wind field from 60° N to 40° S. To study the interhemispheric interactions, a fourteen-year monthly mean wind fields at the surface, 700 mb and 200 mb levels are constructed. As in Shield (1985), we will use the change of the equatorial zonal wind along 10° S as the main parameter to represent the onset of the southern monsoon. The reason for us not to choose the conventional definition of onset, for instance, rainfall or satellite imagery, is: first, that, as a vigorous surge reaches the South China Sea, a belt of strong northeasterly winds forms within 24 h off the South China coast. As a result, the variation of the northern winter monsoon is best represented by the surface northeast winds and it is anticipated that the signal of its possible influences may be more apparent in the surface winds of the southern summer monsoon. Second, the low-level equatorial westerlies are the closest to the equator, and, therefore, it should be the first indicator to reveal any response from the Northern Hemisphere. As defined by Troup (1961) and Davidson et al. (1983), the significance of equatorial zonal wind to be the key parameter lies in the fact that monsoonal westerlies are the prelude to monsoonal rainfall over northern Australia.

The outline of this paper is as follows. We describe the data in section II, and discuss the time mean circulation of wind, velocity potential and streamfunction in detail in section III. Section IV is devoted to the discussion of time variations of the events associated with the monsoonal circulations. Finally , the conclusions are given in section V.

II. DATA AND PROCEDURE

The basic data used in this study are the 200 mb, 700 mb and surface winds for fourteen years (from 1974 to 1988) from the United States Navy's Fleet Numerical Oceanography Center's (FNOC) Operational Numerical Variational Analysis. These data are analyzed twice daily on a tropical global band from 40° S to 60°N by objective procedures on a 49 × 144 Mercator grid having a grid resolution of approximately 2.5° N × 2.5° N . the Mercator secant projection results in a change in the actual distance between grid points from 140 km at 60° N to a maximum value of 280 km at the equator. Unlike many operational objective analysis products, numerical weather prediction is not used to provide first guess. Rather, the six-hour persistence field is used as the first guess. The analysis is a successive corrections technique based on Cressman's (1959) method. The analyzed horizontal fields are also adjusted by a set of numerical variation analysis equations which incorporate the dynamic constraints of the momentum equations, with friction included in the surface layer (Lewis and Grayson, 1972).

The period of study is the 14 Northern Hemisphere winter monsoons (November-February) of 1974-1988. Our attention will be directed to the twice-daily zonal (u) and meridional (v) wind components at the surface, 700 mb, 400 mb and 200 mb. These components are subsequently divided into a rotational part and a divergent part, i.e. ,

$$V = \nabla\chi + \mathrm{K} \times \nabla\psi, \tag{1}$$

where the streamfunction ψ and the velocity potential χ are obtained by solution of the Poisson equations

$$\nabla^2\psi = \zeta = \left(\frac{\partial v}{\partial x} - \frac{\partial u \cos\phi}{\cos\phi \partial y} \right) \sec\phi \quad \text{and} \tag{2}$$

$$\nabla^2\chi = -\delta = -\left(\frac{\partial u}{\partial x} + \frac{\partial v \cos\phi}{\cos\phi \partial y} \right) \sec\phi. \tag{3}$$

Here, ζ is the relative vorticity

$$\frac{\partial v}{\partial y} - \frac{\partial u}{\partial x} \tag{4}$$

and δ is the divergence

$$\frac{\partial u}{\partial x} + \frac{\partial v}{\partial y}, \tag{5}$$

where the horizontal coordinates in the Mercator projection are taken as

$$x = a\lambda \quad , \quad y = a \ln\left(\frac{1 + \sin \phi}{\cos \phi} \right) \tag{6}$$

Here, a is the radius of the earth, and λ and ϕ are longitude and latitude, respectively. Both ζ and δ were approximated using centered differences on the GBA Mercator grid.

As boundary conditions for (2) we assume $\psi = 0$ at 40° S and 60° N. The technique used to calculate ψ is essentially method II of Shukla and Saha (1974). This method uses the previously computed χ field to compute boundary conditions for ψ . The values of ψ are displayed above 50° N although the solution for ψ encountered at this boundary is difficult due to this region being meteorologically active. We assume that the χ and ψ field in the equatorial regions are sufficiently remote from the boundaries such that the values of ψ , χ are not affected by the choice of boundary conditions.

The data base was carefully reviewed to identify missing or errorneous fields. The end result yielded few data gaps. The significant blocks of missing data run from 1) 1200 GMT 06 December 1976 to 1200 GMT 16 December 1976 , 2) 0000 GMT 20 November 1984 to 0000 GMT 31 December 1984. However, for the sake of completeness, we replace those inconsistent or missing data by linearly interpolated values based on the closest adjacent data.

Since most of our discussion will focus on the possible relationship between the northern winter monsoon winds and the southern equatorial monsoon winds, the following data were computed:

- Monthly means of the observed winds, streamfunction, and velocity potential for the surface , 700 mb and 200 mb levels for the fourteen winters
- Area averaged parameters of wind and vorticity whose time variation represents certain circulation features of the monsoons.
- Composited area averaged parameters and composited surface wind field for period of pre- and post- onset of the acceleration of the Indonesian equatorial zonal winds.

III. TIME MEAN CIRCULATION

In this section, we discuss the background features of fourteen-year (1974-1988) monthly mean circulation fields at 200 mb, 700 mb and the surface, which were calculated for the months of November, December, January and February. The variables are wind, velocity potential χ and steamfunction ψ. In general, the fourteen-year mean fields are similar to the nine-year (1974-1983) means examined by Shield (1985).

A. WIND

Throughout the winter monsoon season, three circulation features are particularly relevant. They are : 1) the surface northeast monsoonal winds in the South China Sea , 2) the zonal winds along 10° S from Indonesia-Arafura Sea region extending into Western Pacific, and 3) the Western Australian trough. All can be clearly seen in the monthly mean surface wind (Fig. 1). In November, the northeast monsoon regime has already appeared with a maximum ($>$ 10 m s^{-1}) over the northern region of the South China Sea. In December, the northeast-southwest oriented isotach maximum becomes more extended which indicates the strengthenging of the monsoon winds. This maximum connects the middle and high latitude regions of northeast Asia and Japan with the equatorial South China Sea. Fig. 1 also portrays that the global tropics are covered by the surface northeast trades equatorward of the subtropical ridge. However, the narrow band of the east Asian winter monsoon winds over the South China Sea stands out distinctly as the only regime where the northnortheasterlies extend from middle latitude to the tropics. This suggests that a midlatitude-tropical interaction occurs over the entire region. The isotach maximum weakens in January and February , but the pattern still persists throughout the winter season.

Other features of interest within the Northen hemisphere include the Mongolian high, the northern subtropical ridge along 25° N, and the South Pacific Ocean easterlies. The Mongolian anticyclone (50°N, 93°E) has built up by November as a significant feature and intensifies in December and January. The basic low-level flow in the region of central China and the east China coast are westerlies north of this high center, becoming weak northerlies in the East China Sea and northeasterly through the South China Sea to the Malaysian Peninsula. Within the central North Pacific Ocean, a significant subtropical ridge persists along 25° N, separating the midlatitude westerlies from the northeast trades on the equatorward side. In November, the equatorial zonal flow along 10°

S is generally weak in the vicinity of the Indonesia- Arafura Sea region, but develops into westerlies from December to February. This is an important indicator of the Indonesian monsoon which we will use for the study of the possible relationship between the northern winds and the southern summer monsoons. Also Fig. 1 reveals that, in November and December, the equatorial trough is poorly organized but becomes well defined in January. A confluence zone is centered over the equator in November but migrates south of the equator (5^0 S - 10^0 S) in December.

From inspection of the monthly mean wind field of the 700 mb level (Fig. 2), the following observations can be made: 1) the key features of the surface have either dissipated or reversed at the 700 mb level. The most outstanding feature is the northeasterly monsoonal flow at the surface has been replaced by predominantly westerly winds. The westerly subtropical jet stream is strongest off the northeast coast of China, and the jet stream has its maximum farther west than the maximum at 200 mb (Fig. 3), which is likely due to the upstream topographic influence of the Tibetian plateau. South of the broad westerly winds are easterlies in the Indonesia-Arafura Sea region. There is no evidence of the western Australian low-level cyclone that is observed at the surface, which is consistent with heat low structure. It has been replaced by a weak anticyclone which becomes stronger from December to February, migrating to central Australia.

The fourteen-year mean wind field at 200 mb (Fig. 3) shows that the Northern Hemisphere is dominated by strong midlatitude westerly flow. It has the well - known structure of the two jet stream maxima in the Northern Hemisphere between 20^0 N and 40^0 N : the East Asia jet and the North American jet. In particular, the East Asia jet is obviously the dominant one, with a jet core of 60 ms^{-1} or higher wind centered over Japan, extending from 90^0 E to the dateline. For the North American jet the area enclosed by the 40 ms^{-1} isotach covers only the southeastern United States, about 30^0 in longitude. On the other hand, in November, Southern Hemisphere flow has a wind maximum (>30 ms^{-1}) over central Australia, which extends into the central South Pacific Ocean. It weakens in December. Furthermore, generally weak easterly flow is found in the broad region of the Indian Ocean, maritime continent and western equatorial Pacific Ocean, and South America.

B. VELOCITY POTENTIAL AND STREAMFUNCTION

In this section, we turn our attention to the rotational and divergent components in tropical - midlatitude interactions by examining the time mean charts of velocity poten-

tial χ and streamfunction ψ. As pointed out by Chang and Lau (1980) and Davidson (1984), variations of the divergent wind may cause the changes in convection. According to the equations described in section II, it can be seen that maxima (minima) in values of χ correspond to divergence (convergence) centers. Divergent flow emanates from high χ centers to low χ values and its strength is proportional to the gradient of χ. For those positive χ centers at upper level, one can infer that there is a deep rising motion in the troposphere; Similarly, one can say that at lower levels, convergence represents large scale rising motion.

The nondivergent part of wind field can be expressed in terms of the variations in the streamfunction ψ. The sense of rotational flow for a maximum ψ center is clockwise in the Northern Hemisphere; so, maxima (minima) of ψ correspond to centers of anticyclonic (cyclonic) flow in Northern Hemisphere (equation 2).

The monthly mean velocity potential χ for the surface (Fig. 4) shows a broad area of tropical convergent flow between 10° S and 10° N centered over the east - west oriented maritime continent, extending longitudinally in both directions. The convergent area covers an approximate 150° longitudinal span from the central Indian Ocean to the mid-Pacific Ocean. Another feature in the spatial χ distribution worth noting is the zone of convergence maximum which is centered over the equator in November and December. This zone migrates south of the equator to lay over northern Australia and New Guinea in January and February. .This maximum surface convergent zone is basically oriented in an east-west direction, which is different from the west-northwest to east-southeast tilt of the South Pacific Convergence Zone (SPCZ) shown in satellite pictures. Another area of significant convergent center is found over the northern portion of the South America.

Fig. 4 also shows the significant divergence zone at the surface is located over China and Mongolia extending into the East China coast. It has two maxima throughout the winter season. One is over the east coast of China and the other is over Mongolia , just southwest of Lake Baikal (45° N , 93°E). It should be mentioned that since the artificial boundary conditions imposed may influence the region within about 10° from the northern boundary, this Mongolian divergent maxima may actually be located slightly to the north by a few degrees. Other areas of significant divergent centers are found in the eastern areas of the North and South Pacific Oceans and in the southern Indian Ocean.

In December and January, the north - south component of $\nabla \chi$ intensifies between 100° E - 140°E. It is important in the overturning motions. This is indicative of the

lower branch of the local East Asia Hadley cell. And, we will combine with 200 mb charts to present an overview of three - dimensional planetary - scale circulation in the following discussion.

The 700 mb χ field (Fig. 5) clearly shows that there exists two significant divergent centers, one is over northeast China and the other one is over equatorial central Pacific Ocean. In between these two divergent centers, the South Pacific Convergence Zone (SPCZ) is centered on the equator from the Celebes Sea to the central South Pacific Ocean with a west-northwest to east-southeast orientation. This convergence zone, although distinctly weaker than at the surface, expands and intensifies throughout the season. In comparison, the data of Oort (1983) shows a sharp reduction in the magnitude of the divergence over the African and South American convection centers when going from the surface to the 700 mb level but it is not as great as indicated by Fig. 5.

For all the winter season, the mean velocity potential χ at 200 mb level (Fig. 6) shows a vast region of tropical divergent flow centered over the east-west oriented maritime continent of Indonesia and Borneo with a small secondary maxima further to the east (near 180°E) in November. The divergent center extends longitudinally in both directions. To the east-southeast, the central axis extends deeply into the tropical southeastern Pacific, representing the outflow of the SPCZ. To the west and west - southwest, it extends to tropical South Africa covering the equatorial Indian Ocean. Another region of a significant positive χ center is found over the northern part of South America, extending into the equatorial Atlantic.

As revealed in Fig. 6, the streamlines of divergent flow emanating from positive χ centers again show that both north - south and east - west components are important. According to the assumptions described in section II, these centers indicate large scale rising motion in the troposphere which is most likely due to the presence of condensation heating. Coupled with the mean fields of the lower levels, it can be easily seen that parts of the divergent flow originating from the South China Sea and maritime continent subside over Eurasia with the maximum 200 mb convergence centered in northwest China. The ascending motion over the maritime continent, coupled with descending motion over Eurasia, constitutes a strong local Hadley cell which occupies a longitudinal belt from East Asia to the western Pacific. Also the east - west gradient of the isopleths shows the divergent flow stretch along the equator in both directions to form two Walker cells. The eastern Walker cell extends to the equatorial western Pacific with a descending branch in the equatorial central Pacific. On the other hand, the

western Walker cell extends across the Indian Ocean and Arabian Sea with a descending branch over the east coast of Africa.

In the monthly mean ψ field for the surface (Fig. 7), the most outstanding feature is the presence of a strong subtropical ridge with an east-west orientation, centered at approximately 30^0 N to 40^0 N. The subtropical ridge, with one maximum center over northwest China and the other two centers over the central North Pacific and North Atlantic Oceans, separates the lower tropospheric midlatitude westerly regime and the tropical easterly regime. Another feature in the streamfunction distribution at the surface worth noting is the presence of the Mongolian high with a maximum ψ center over northwest of China. The Mongolian high, with its obviously defined northwest to southeast orientation, intensifies through the winter, indicating a penetration of midlatitude air into the tropics along the east coast of China. This implies the increased northeasterly winds are primarily due to the rotational part of the wind as pointed out in the previous section. During the same period, the western Australian low intensifies and the vorticity trough expands, migrating southward toward the equator until it encompasses the maritime continent region.

Fig. 8 and 9 show the monthly mean ψ fields for 700 mb and 200 mb. A prominent anticyclone to the northeast of the South China Sea in the western North Pacific south of Japan is observed. It is centered at approximately 25^0 N , 162^0 E, and exhibits a somewhat east-west orientation extending eastward into north-central Pacific and westward to eastern Africa. North of this anticyclone is a cyclonic center north of Japan which is separated from the anticyclonic center by a westerly subtropical jet stream extending from northwestern Tibet to the north central Pacific at 200 mb. Note that maxima (minima) in the North (South) Hemisphere are indicated by solid (dashed) lines. South of this anticyclonic center is another anticyclone center (Southern Hemisphere, ψ minimum) with an easterly zonal flow over the maritime continent separating the two centers. Similar north-south distributions of cyclonic and anticyclonic centers, although less prominent, are found over the continents of North and South America, and Europe and Africa. At 700 mb, the 200 mb features west of 120^0E are replaced by the ridge over the Tibetian area which is likely due to the result of topographic effects. Fig. 8 also depicts an anticyclonic center over northern Australia with an easterly zonal flow as at 200 mb.

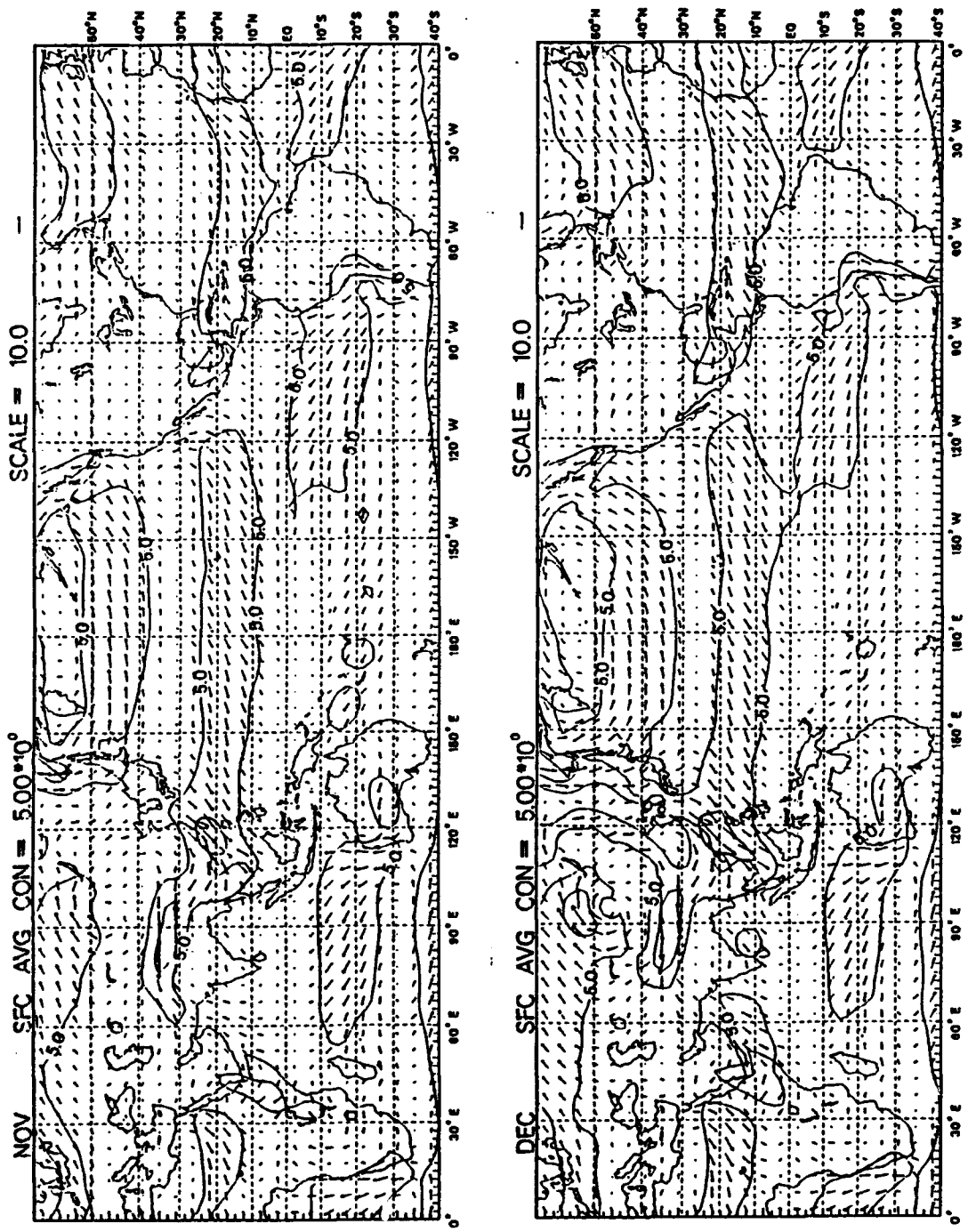

Fig. 1. Latitude-Longitude sections of 14-year monthly mean-surface wind vectors and isotachs.

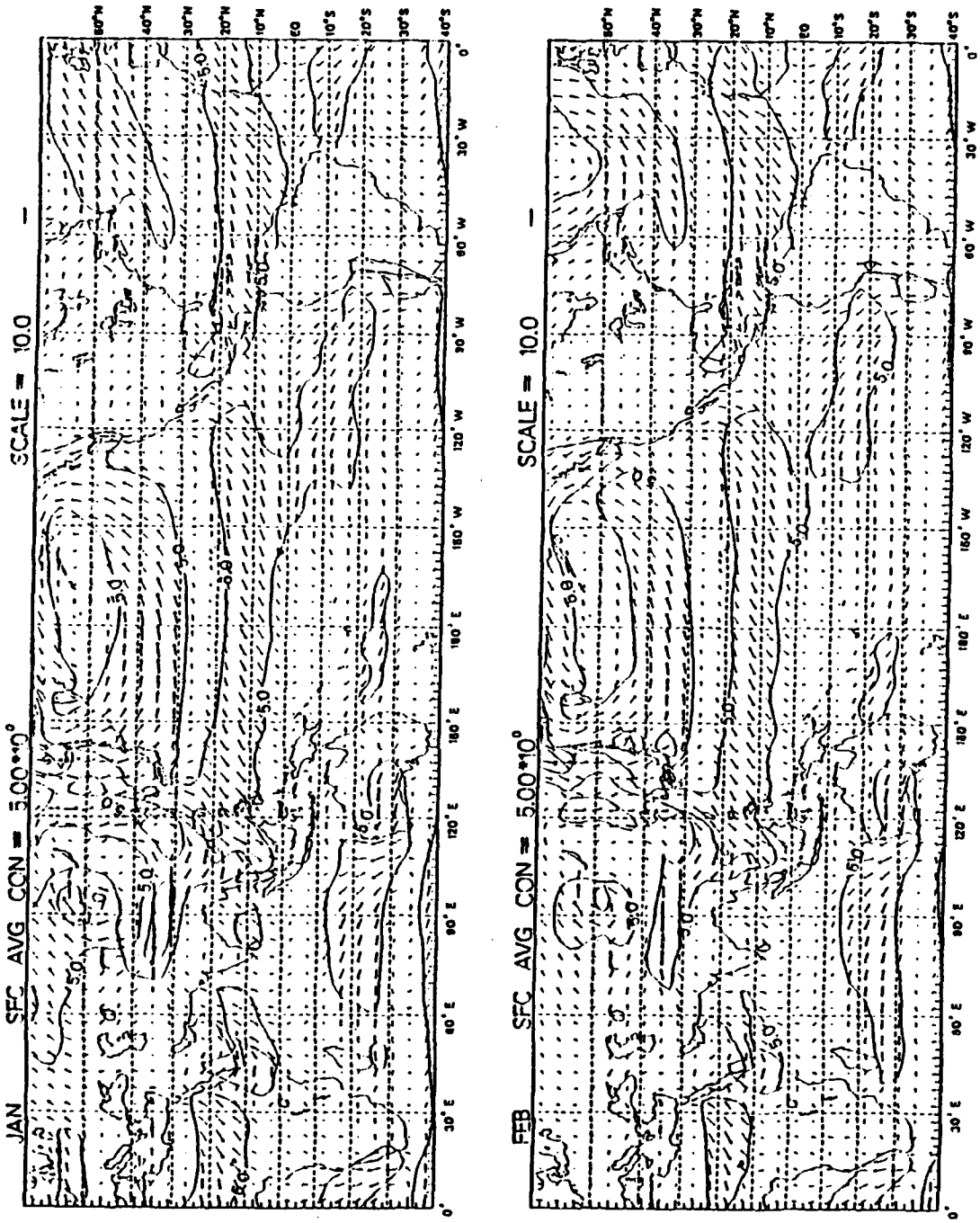

Fig. 1. (Continued)

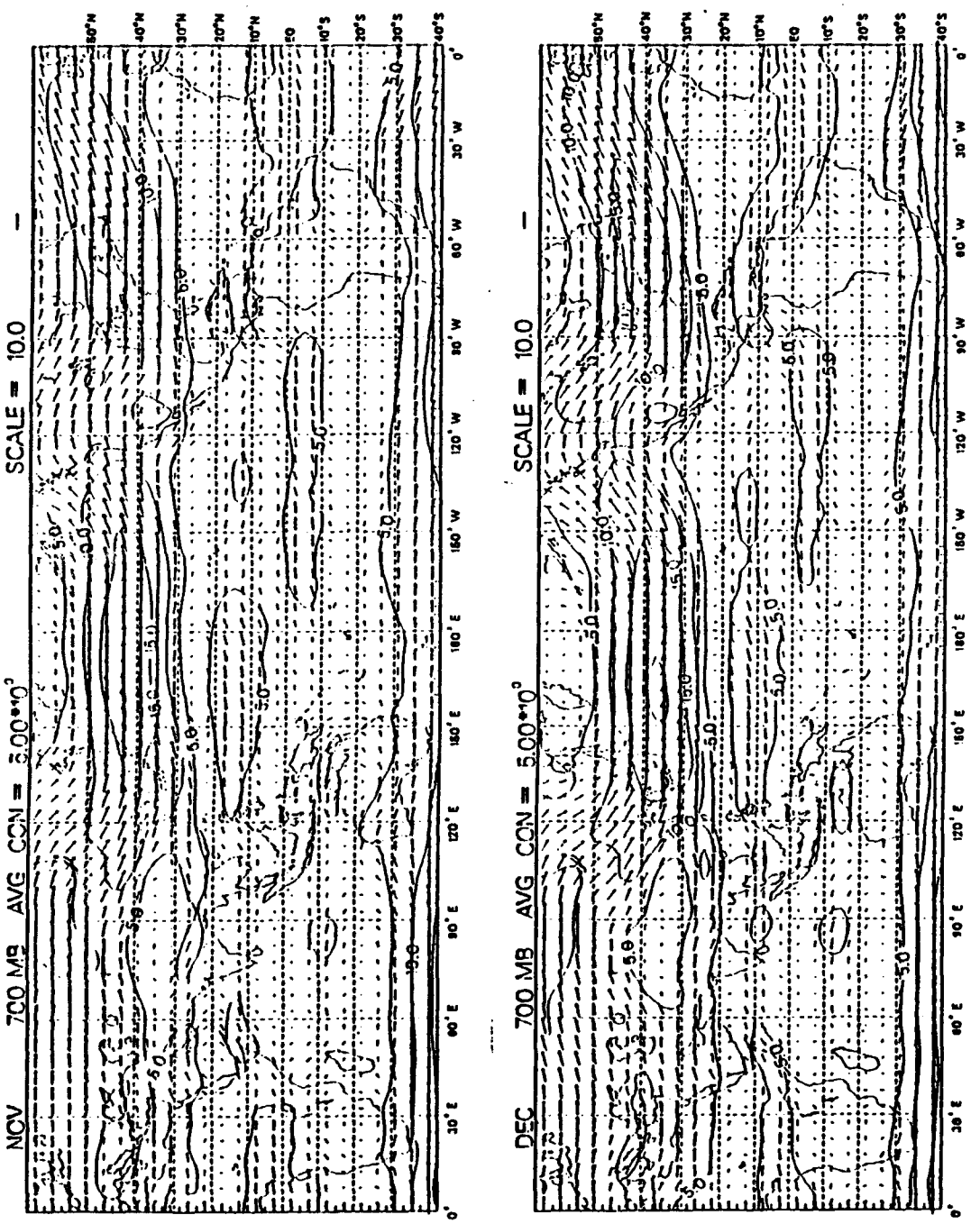

Fig. 2. As in Fig. 1, except for 700 mb level.

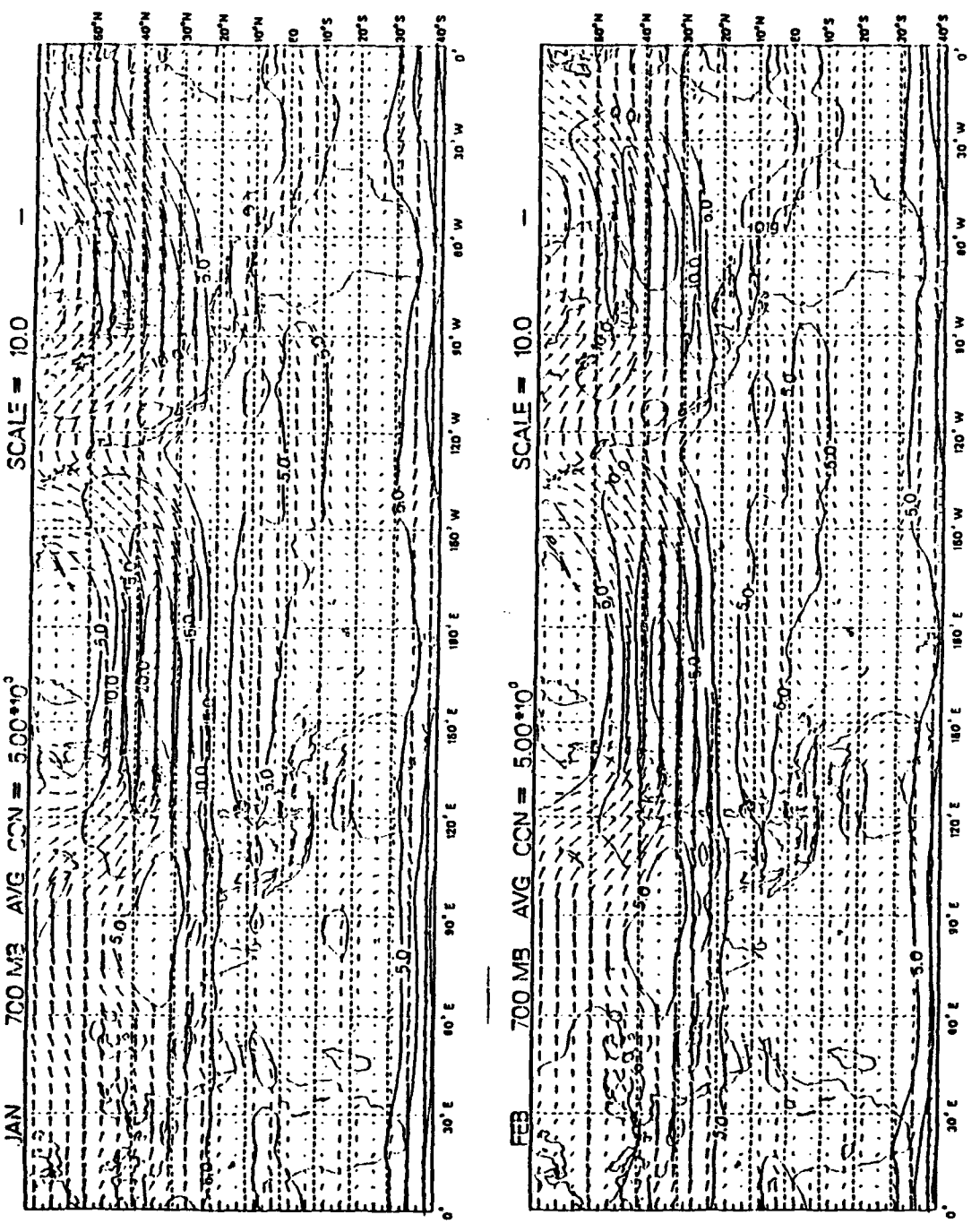

Fig. 2. (Continued)

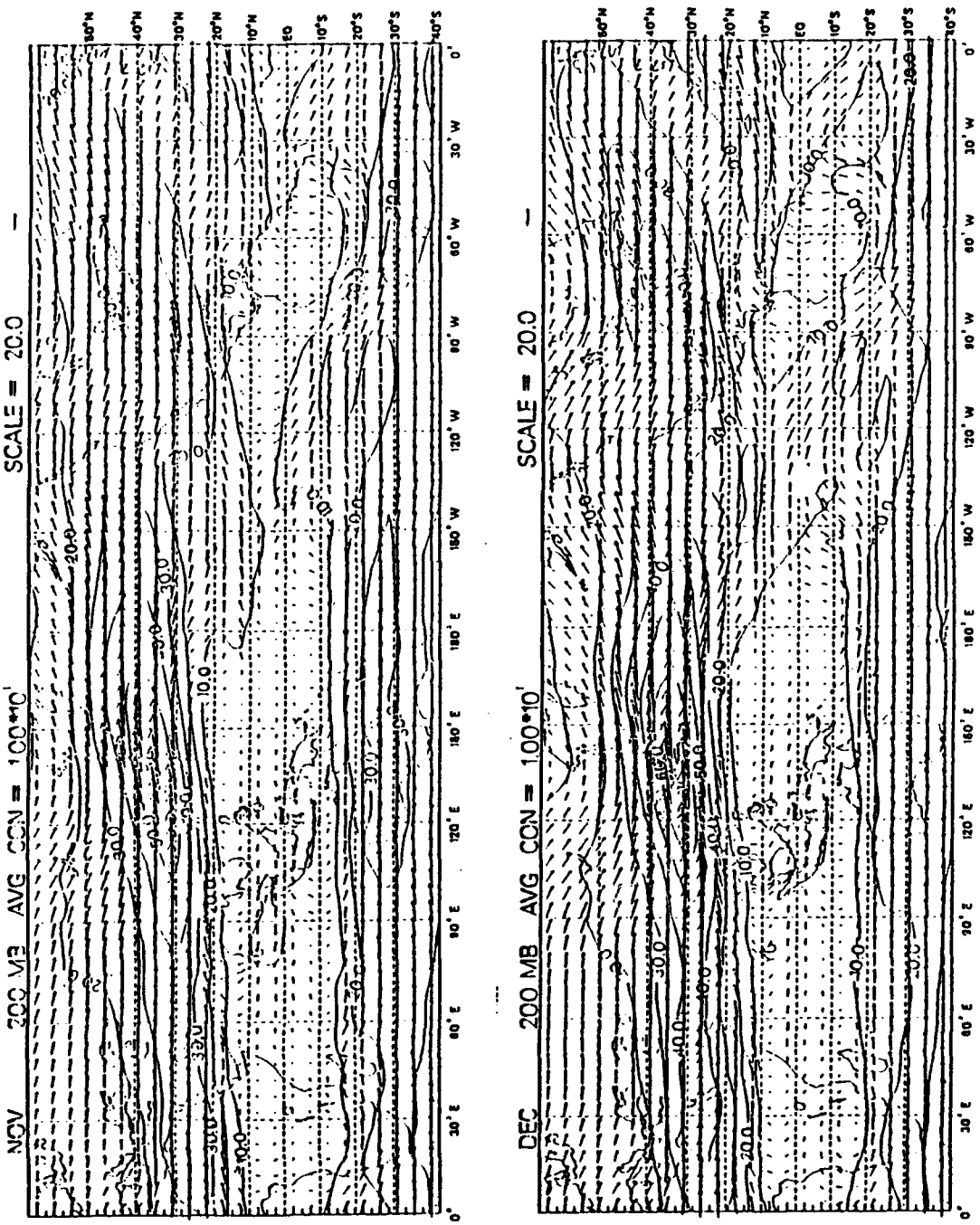

Fig. 3. As in Fig. 1, except for 200 mb level.

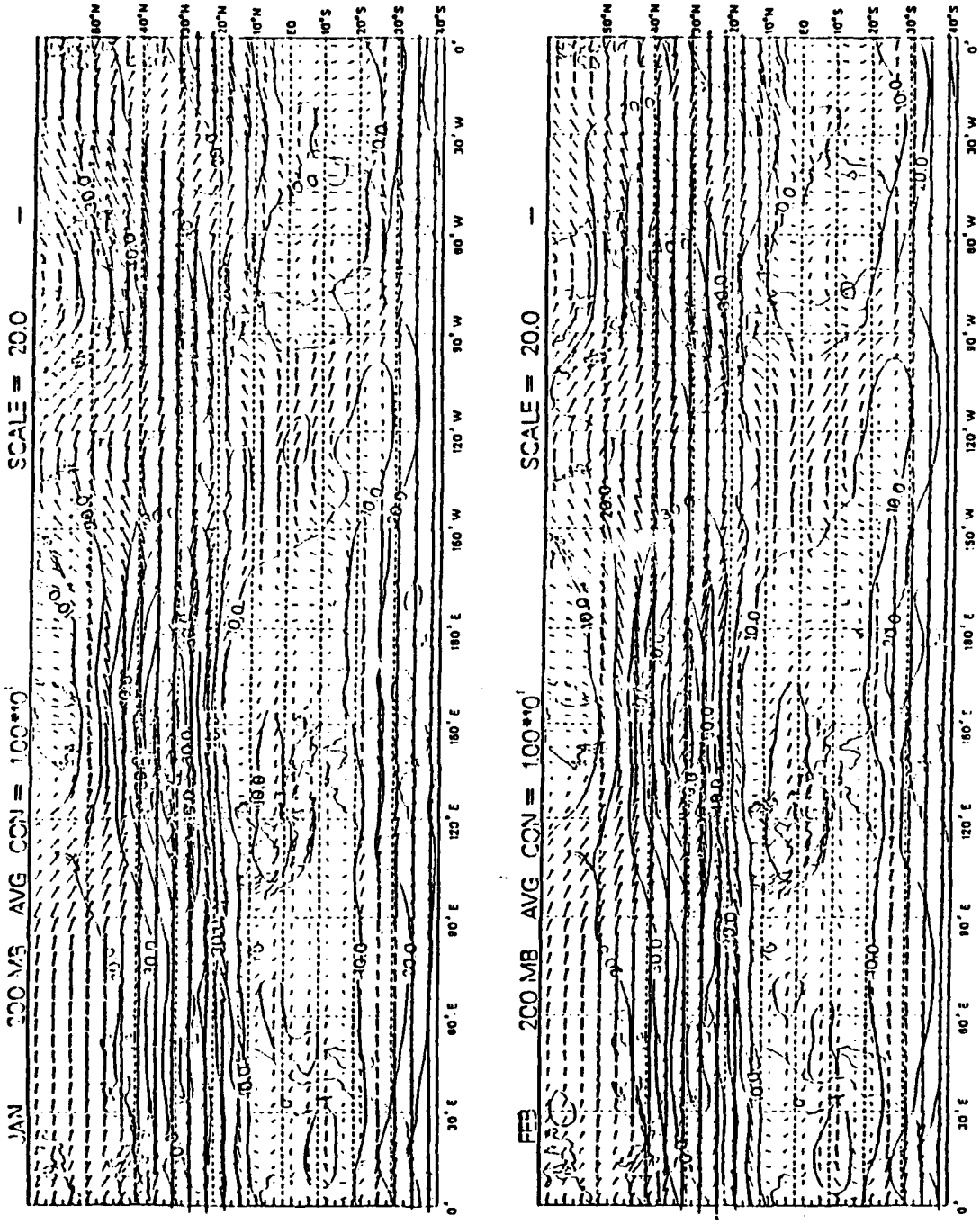

Fig. 3. (Continued)

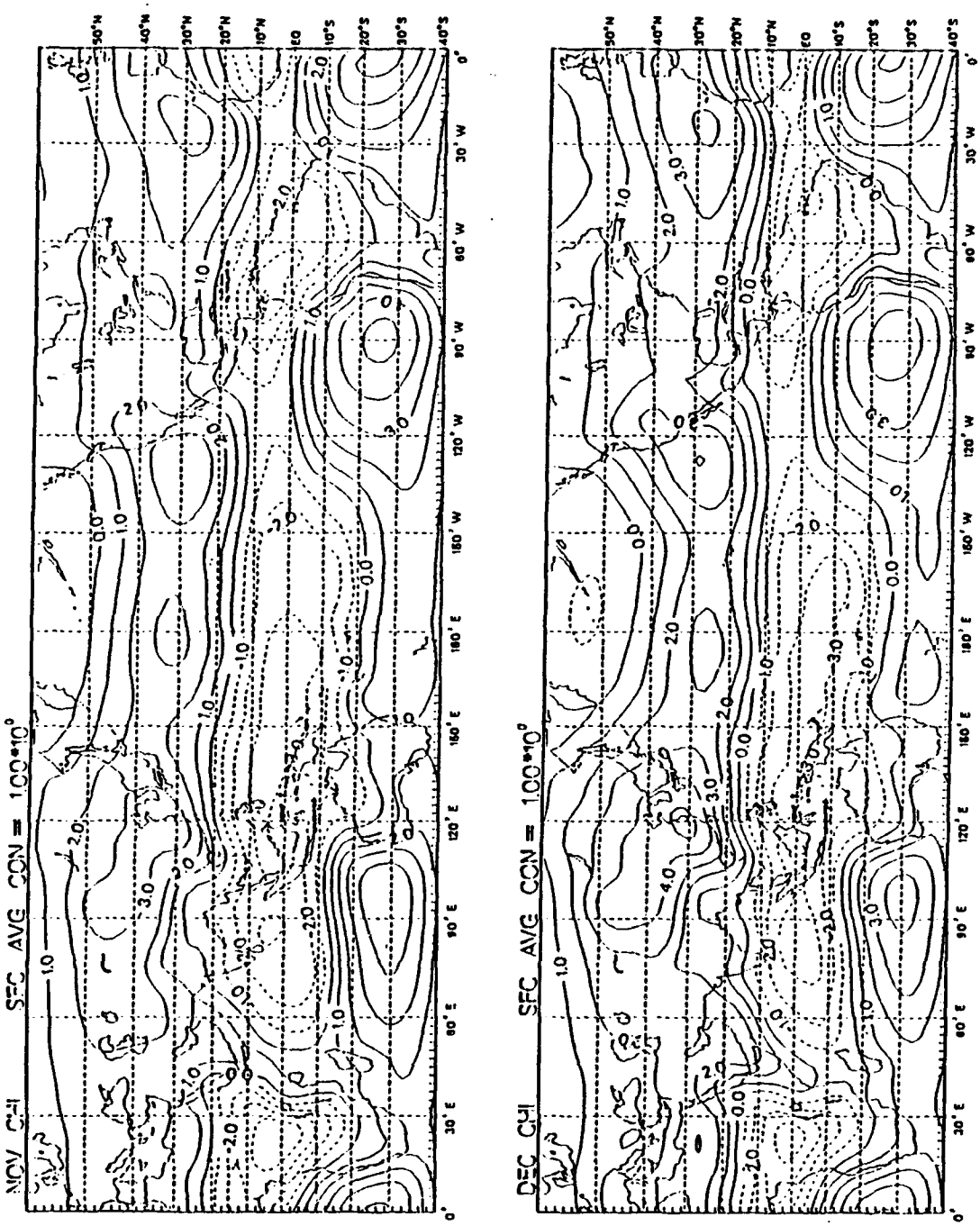

Fig. 4. Latitude-longitude sections of 14-year monthly mean surface velocity potential. Positive (zero) values are solid.

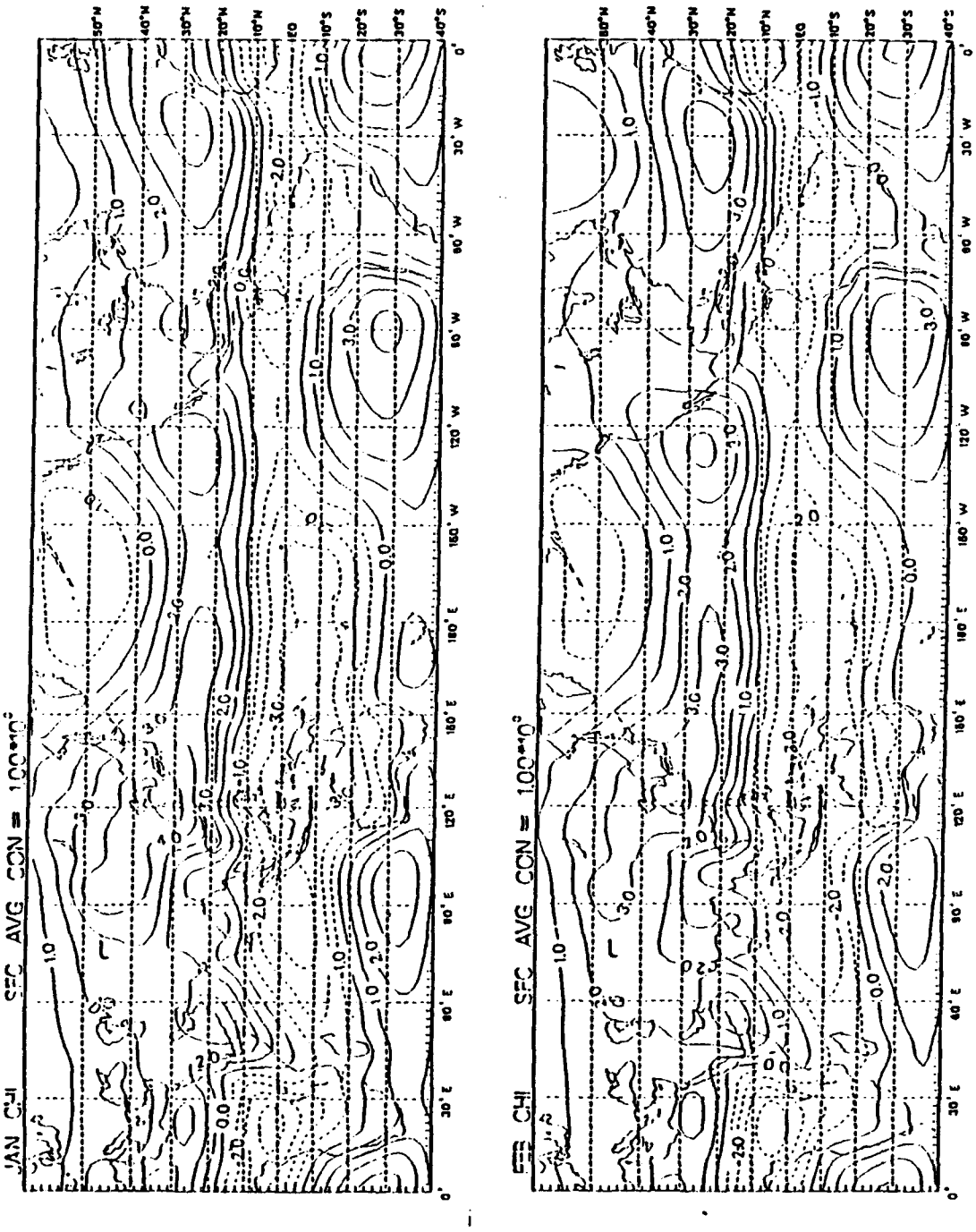

Fig. 4. (Continued)

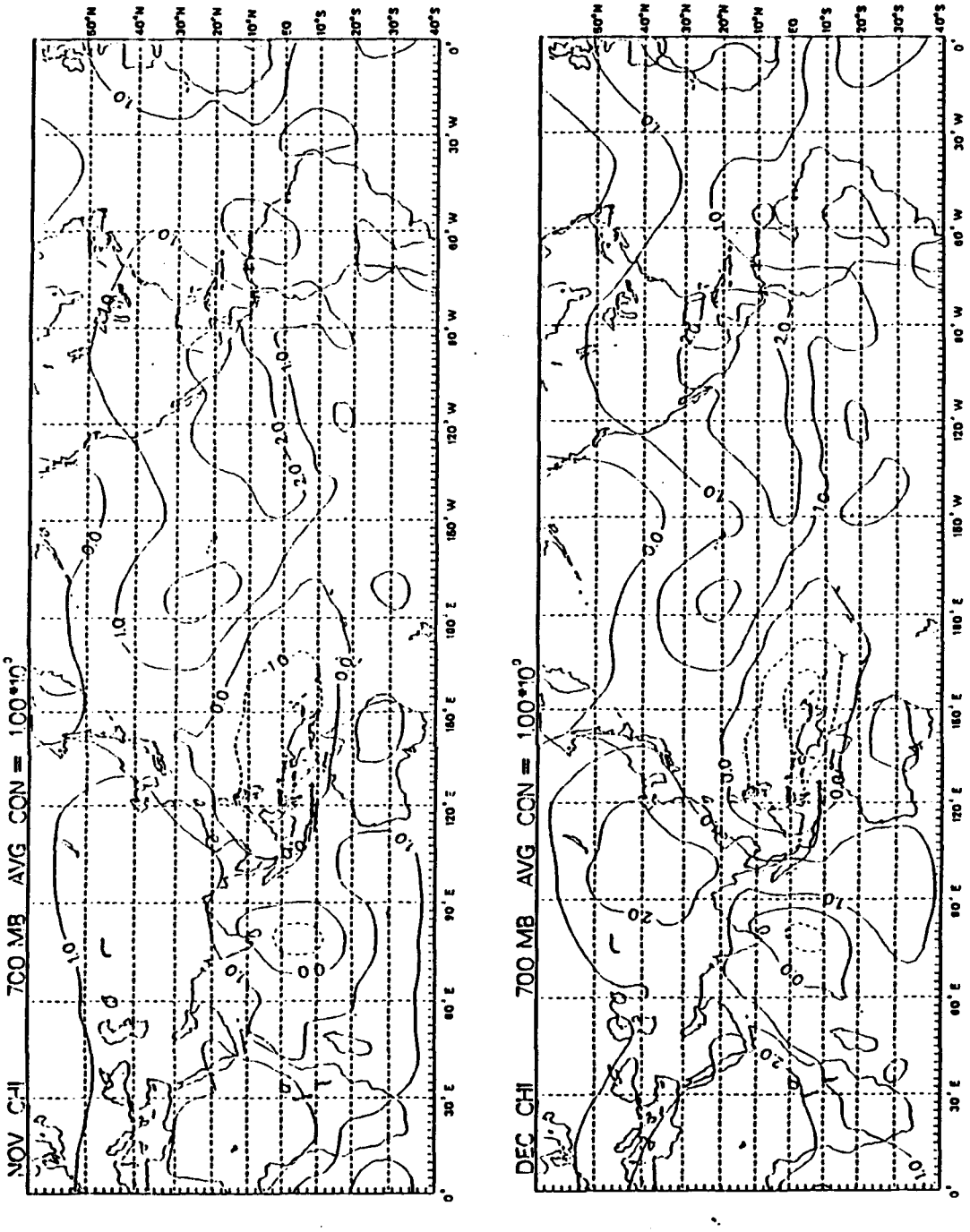

Fig. 5. As in Fig. 4, except for 700 mb level.

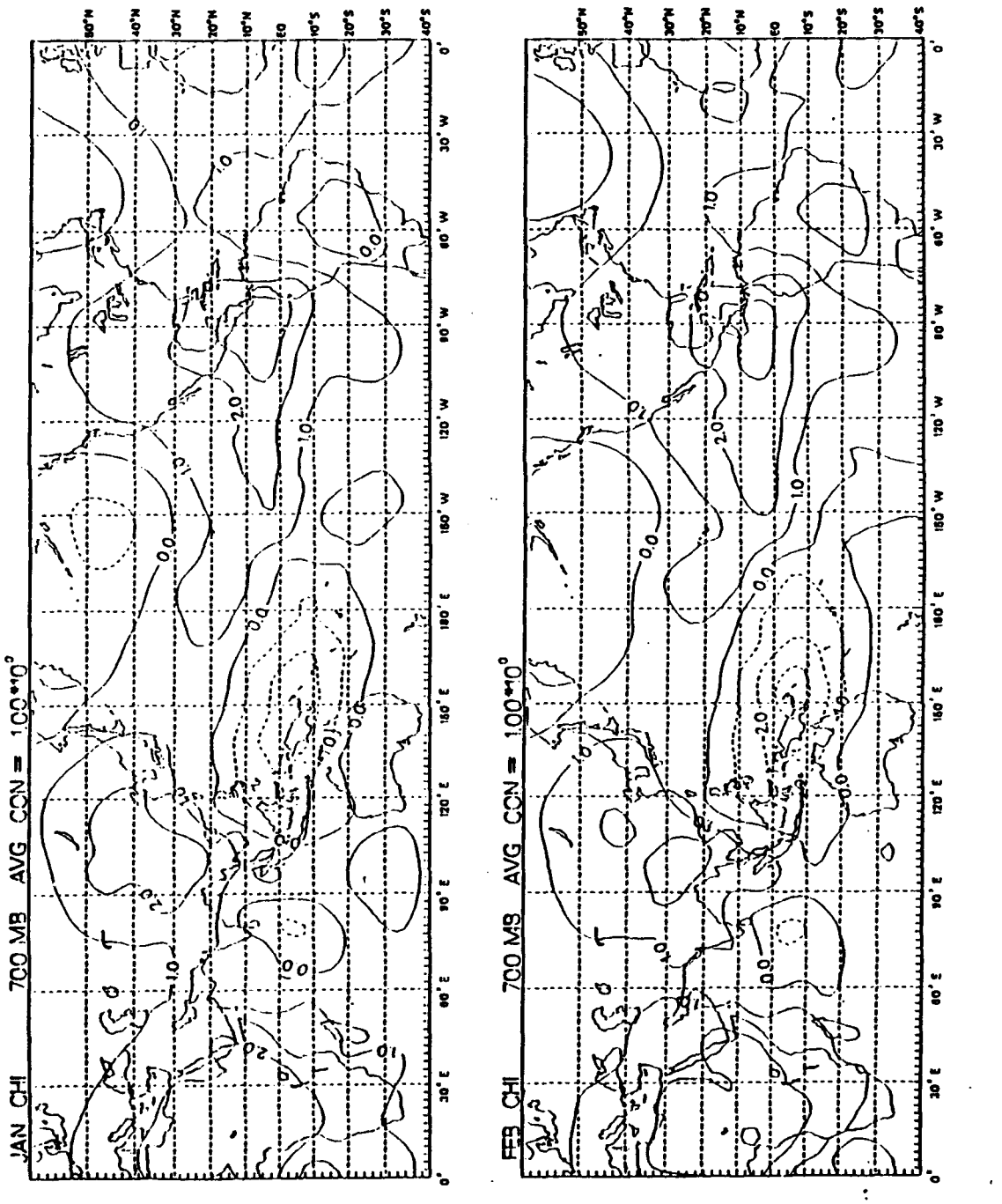

Fig. 5. (Continued)

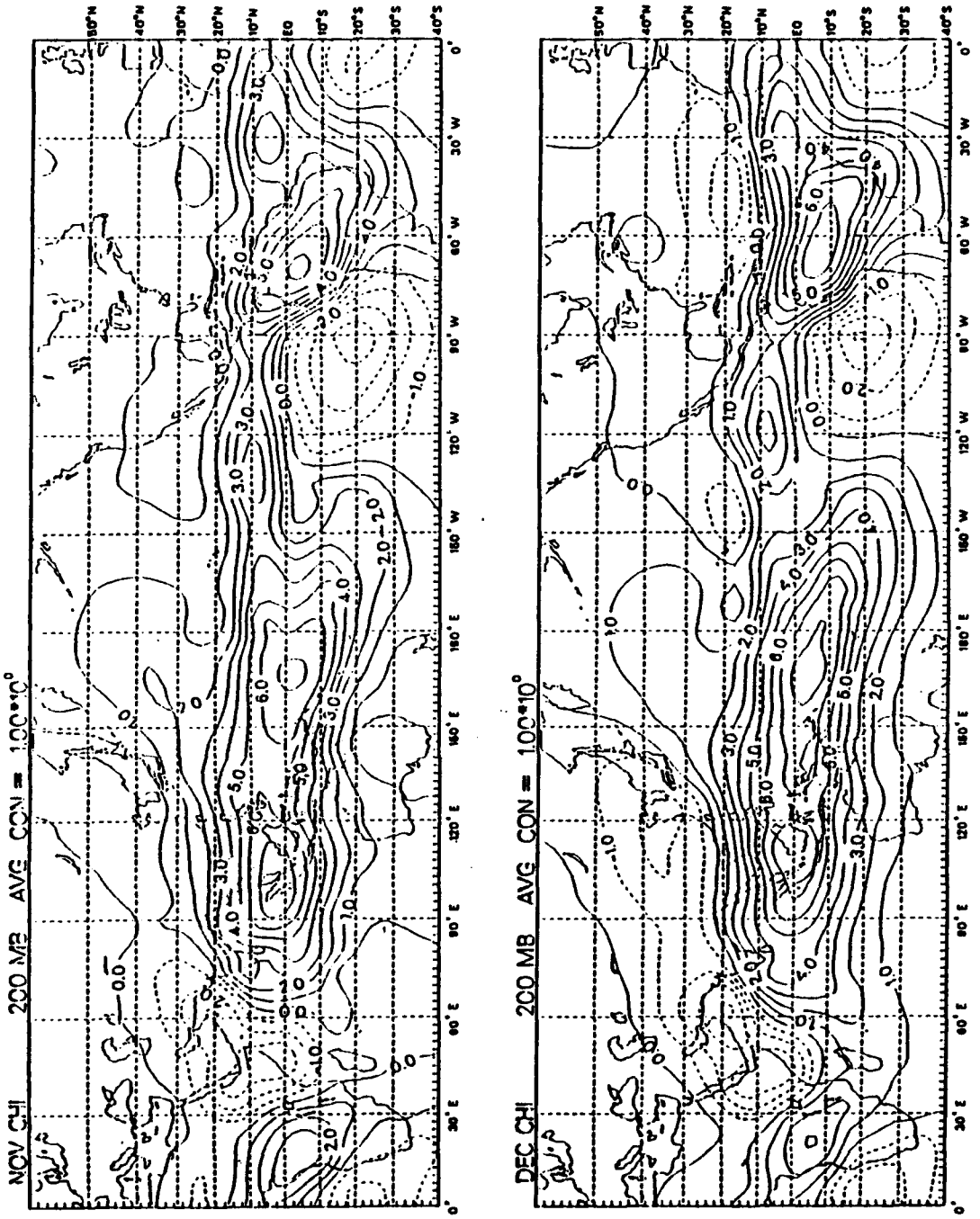

Fig. 6. As in Fig. 4, except for 200 mb level.

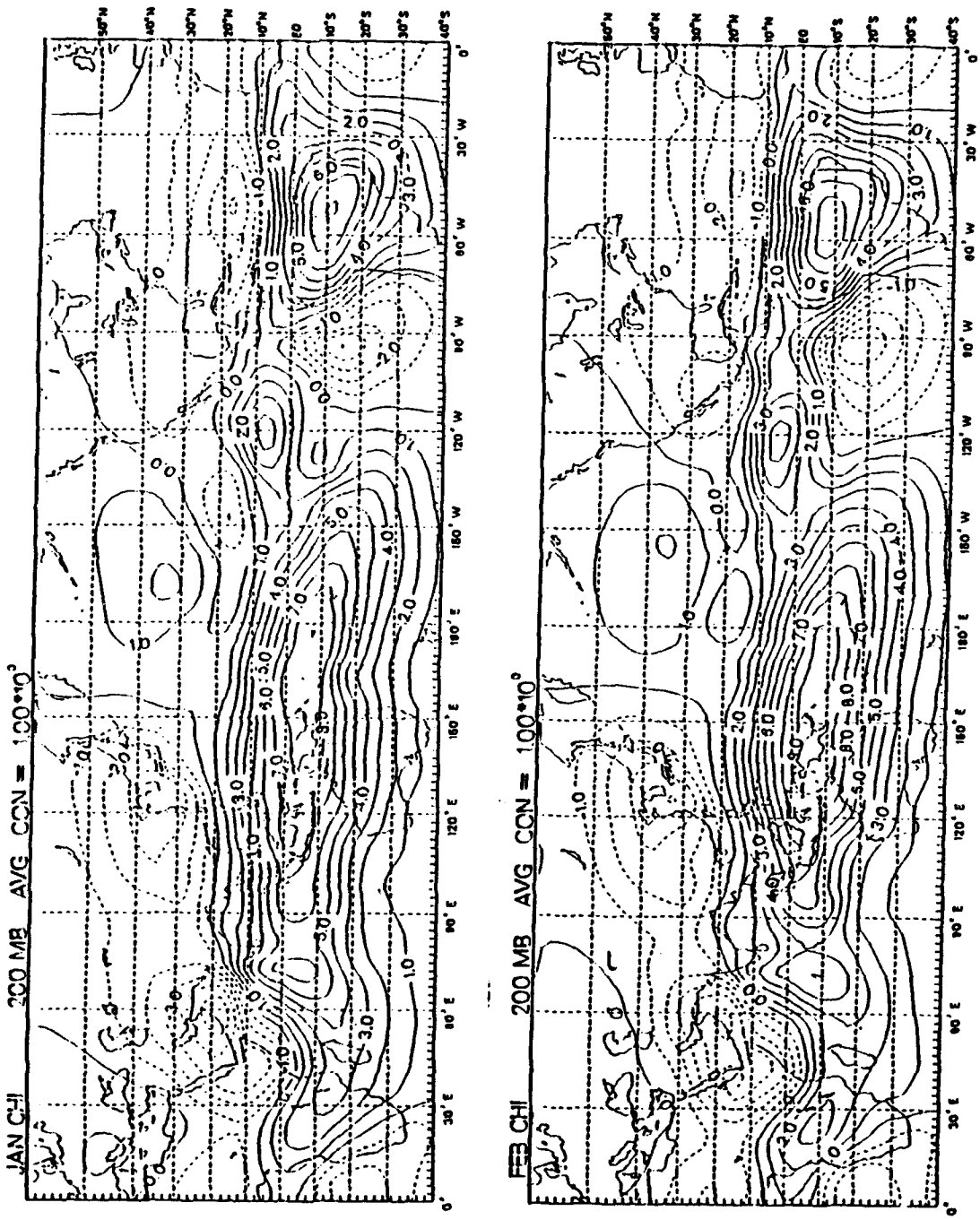

Fig. 6. (Continued)

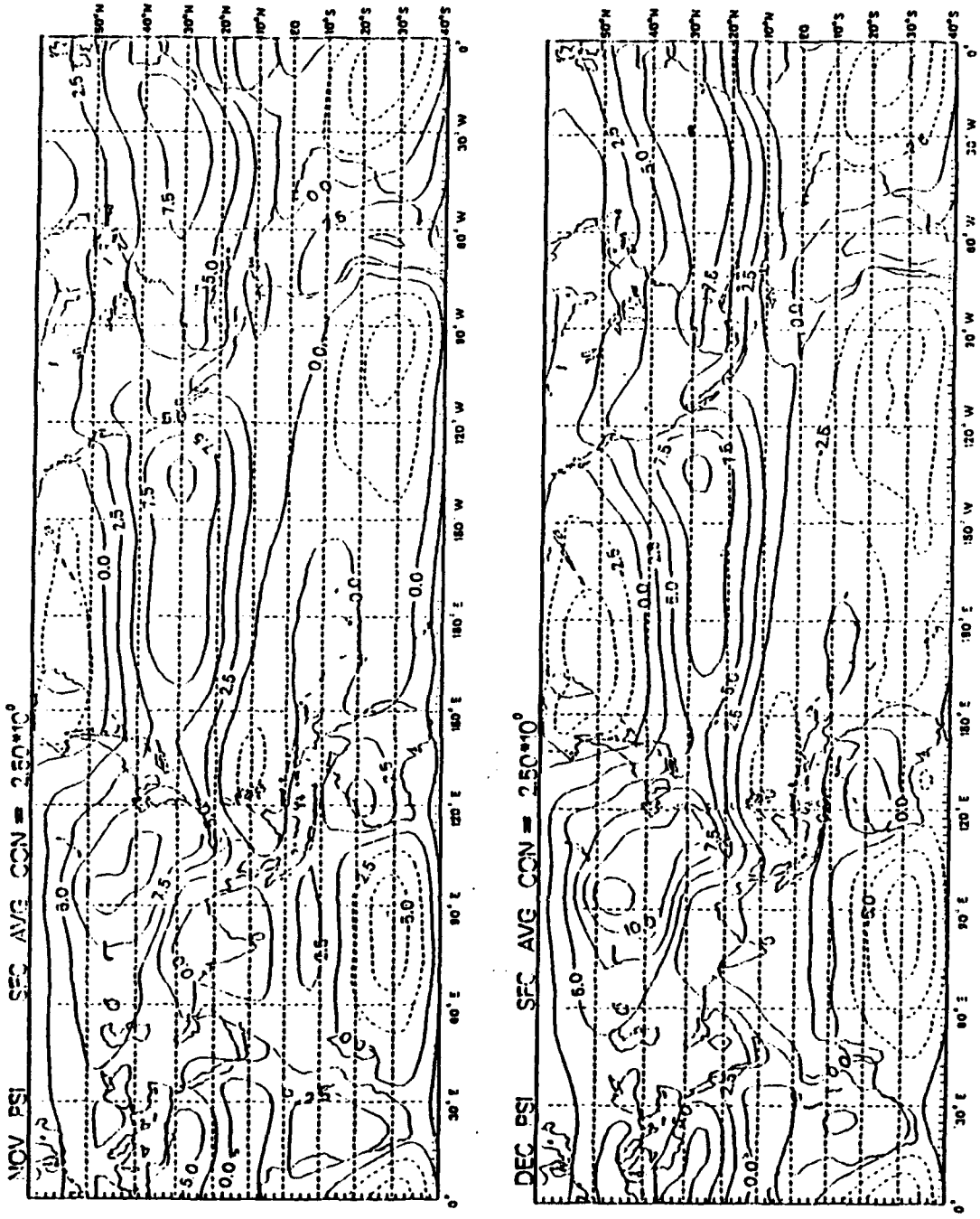

Fig. 7. Latitude-longitude sections of 14-year monthly mean surface streamfunction.

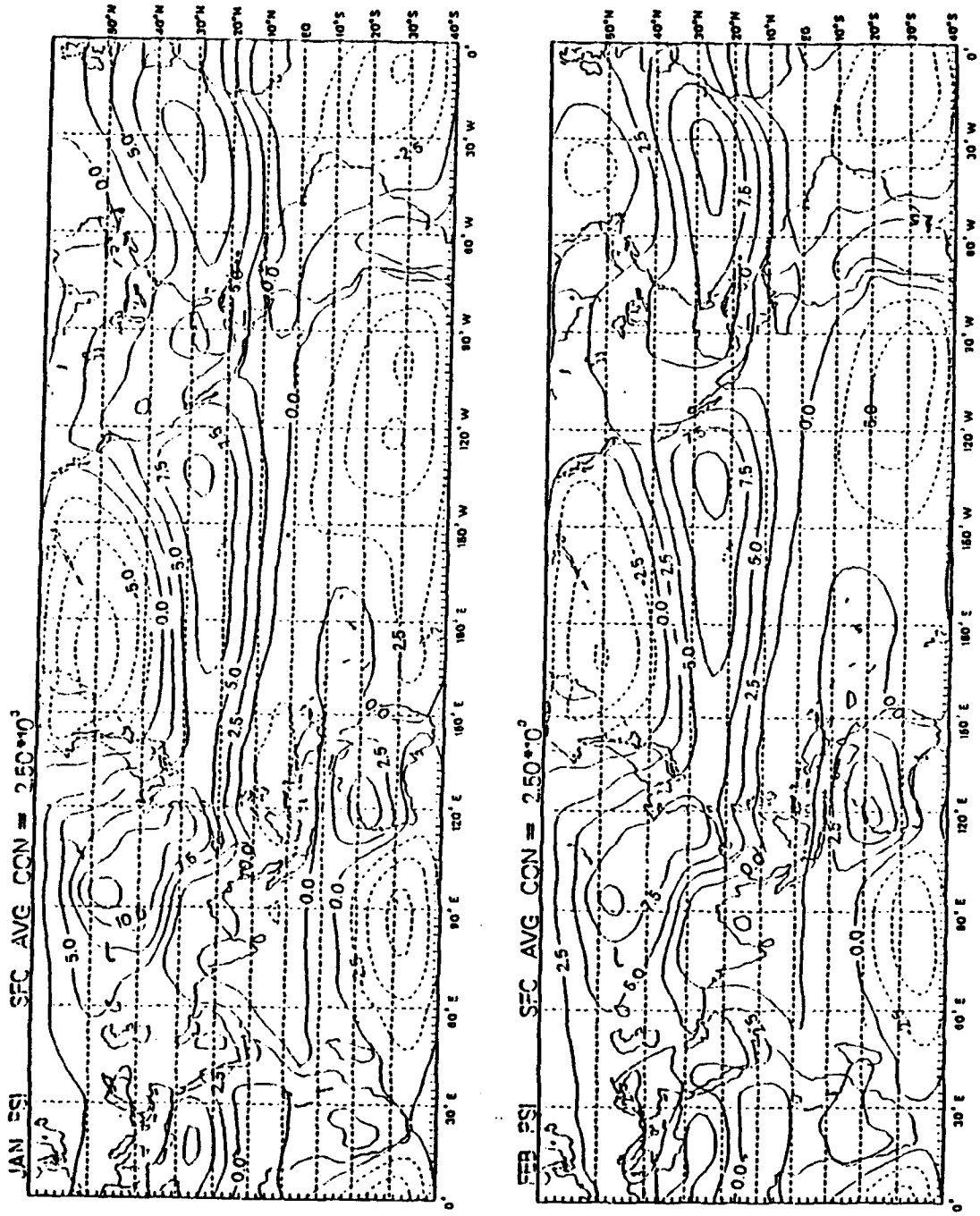

Fig. 7. (Continued)

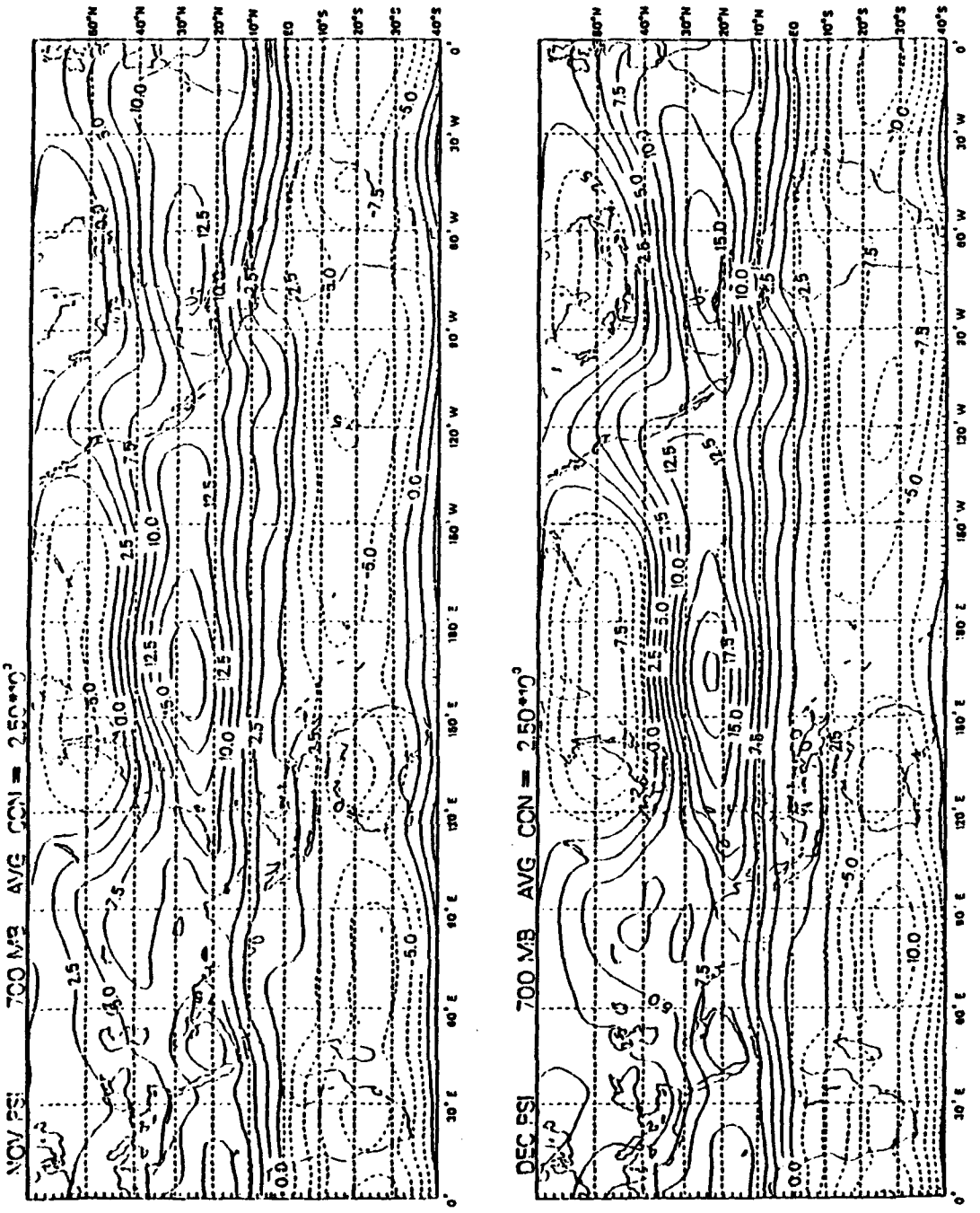

Fig. 8. As in Fig. 7, except for 700 mb level.

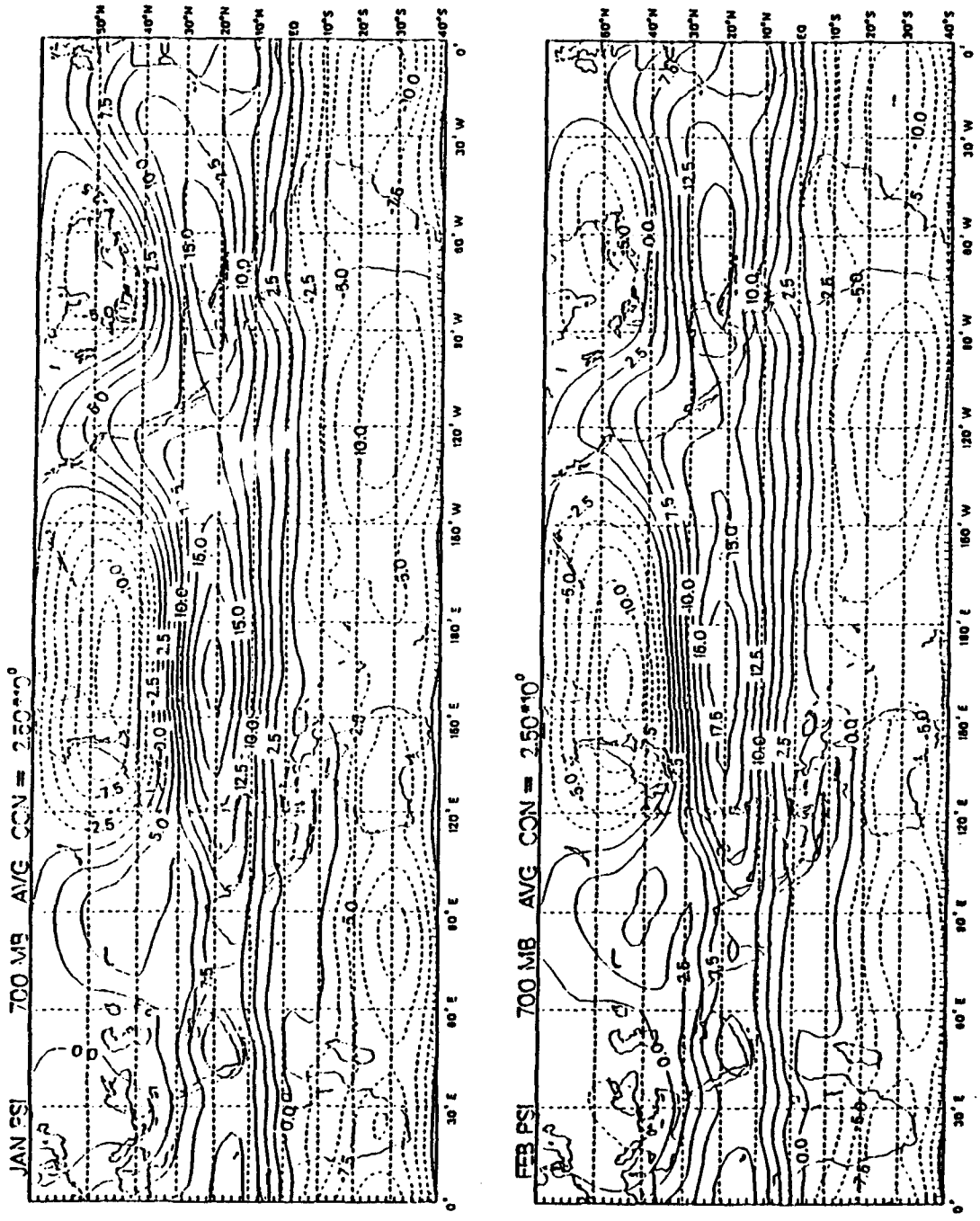

Fig. 8. (Continued)

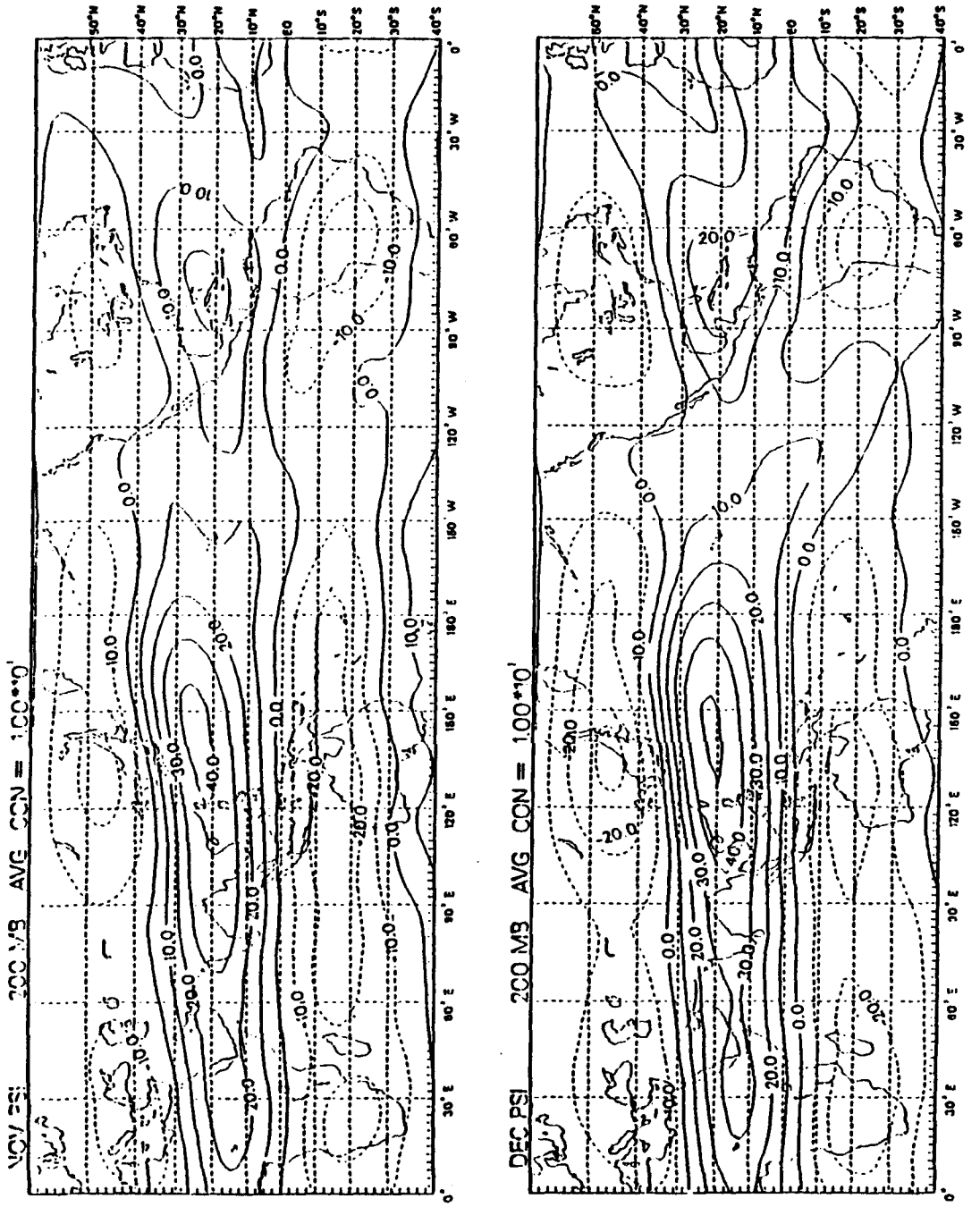

Fig. 9. As in Fig. 7, except for 200 mb level.

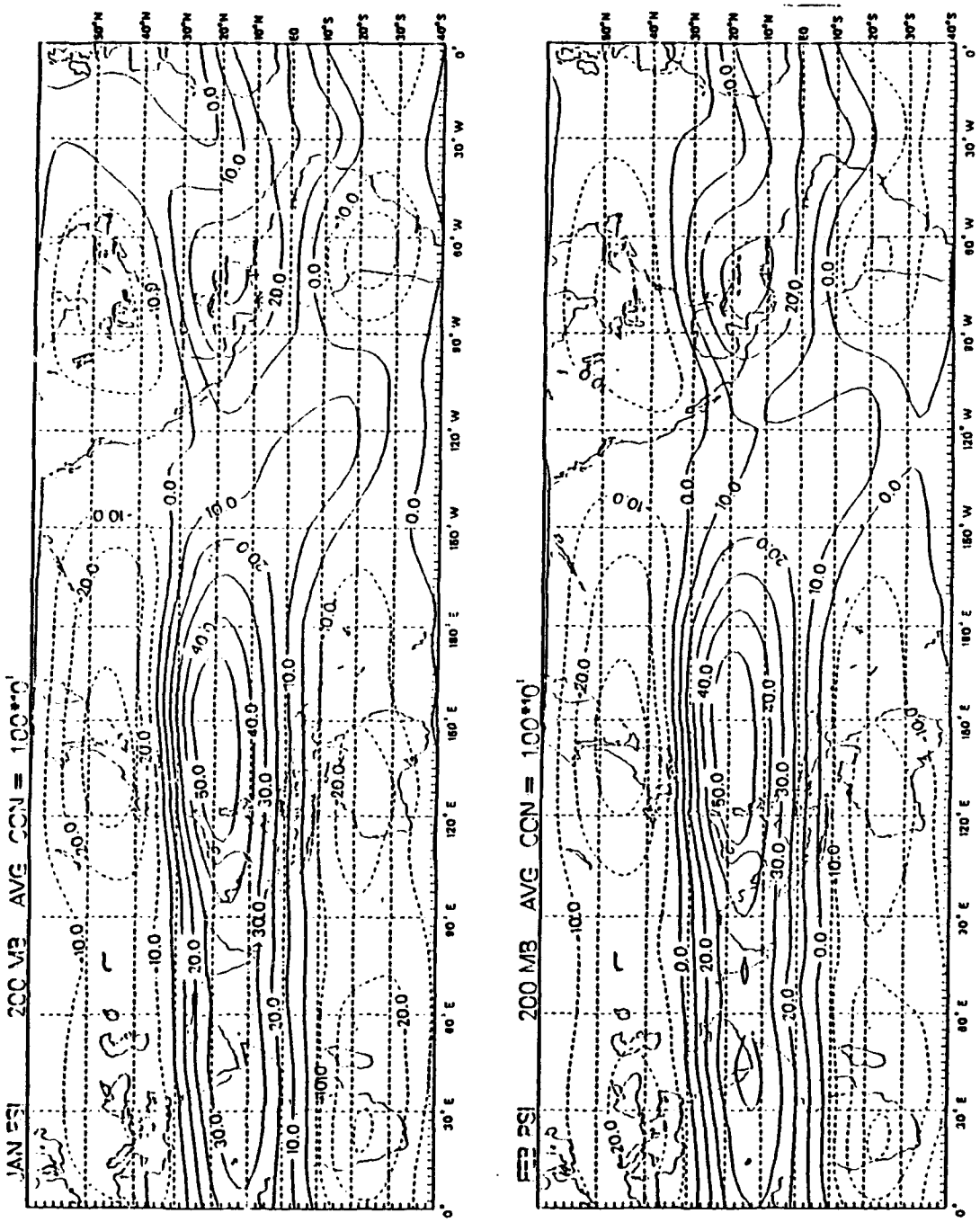

Fig. 9. (Continued)

IV. TIME VARIATION OVER THE MONSOON REGION

A. COMPOSITE TIME SERIES

To examine in detail the possible interaction between the northeast monsoon in the Northern Hemisphere and the South Hemisphere's summer monsoon, the time series of eleven surface large-scale circulation parameters averaged over selected regions for the entire winter season are constructed. Selected horizontal motions in these regions, considered to have a possible relation with the development of the equatorial monsoon winds along 10° S, are defined as the circulation parameters. The selected regions and parameters are shown in Fig. 10. Here in regions NEM1, NEM2 and NEM3 the parameters representing winter monsoon surges are the surface meridional wind over northern part of South China Sea (includes Taiwan, Philippine Islands and Guam) ; in regions XEF1, XEF2 and XEF3 the parameters representing cross equatorial flow are the surface meridional winds over the maritime continent and equatorial Pacific Ocean; in regions SSM1, SSM2 and SSM3 the parameters representing equatorial monsoonal flow over Indonesia-Arafura Sea region are the surface zonal wind; in region WAT the parameter is the surface vorticity over northwestern Australia, and in region SHM the parameter is the 400 mb vorticity over southwestern Australia. Table 1 lists these parameters, circulation components, as well as their respective areas. The choice of these parameters is based on the monthly mean flow patterns described in the preceding sections. In order to examine the time variation of these eleven parameters, we calculate area averages for each of these parameters twice daily.

In this study the basic parameter used as the index to determine the timing of the major circulation changes with respect to the change of equatorial westerly flow is SSM1. Again, from Table 1 and Fig. 10, SSM1 represents the area-averaged zonal wind component of the surface winds over the Indonesia-Arafura Sea region (12.5- 7.5° S, 115- 135° E). As hypothesized earlier, as a cold surge reaches the South China Sea, a belt of strong northeasterly wind will form right off the south China coast. This may instigate a cross-equatorial flow and influence the surface winds of the southern Hemisphere. Furthermore , the low-level equatorial westerlies are the closest to the equator, and it should be the first indicator to reveal the forcing from the Northern Hemisphere. These are the reasons SSM1 is used as the basic index , and from it we can construct the basic time series which defines the timing of events.

From inspection of the time series of SSM1 for each of the fourteen years, the following observations can be made: 1) there are several significant fluctuations in the zonal winds throughout the winter months. 2) there are also diurnal fluctuation phenomena in the time series. Based on the fact that the onset of the summer monsoon usually occurs near the end of December, we focus on the major events occurring after 15 December for each year. As used by Shield (1985) the condition for an event to be chosen as an onset event is that there is a period of continuous acceleration of more than five days which occurs after 15 December. The initiation of the onset event is the relative minimum preceding the period of five-day sustained acceleration. Fig. 11 shows the time series of SSM1 for 1974-1975. The abscissa represents dates from 1 November to 31 March. As shown in Fig. 11, the two onset events can be readily seen in the zonal wind series. The first event starts from 07 January 0000 GMT; it will be called the " mid-season " event. There is often another major acceleration event after the mid-season event which will be called the " late-season " event. Fig. 11 shows the late-season event that starts from 06 February 0000 GMT. There is inevitably some subjectivity in choosing the dates of these events. Since some seasons did not experience a break in southern monsoonal flow, only nine years were chosen as having late-season onset events. Besides this, we do not choose the mid-season onset for 1984-85 and 1986-87 simply due to missing data. Thus, only twelve years were chosen as having mid-season onset events. Table 2 gives the specific date and time selected for TAU = 0 (onset) for each year for both the mid- and the late-season events.

As noted earlier, in this study we use SSM1 as base series to determine the initiations of the onset events. Based on the time of TAU = 0 for both mid-season and late-season events for each year (shown in Table 2), each area-averaged circulation parameter was composited from TAU = -5 days to TAU = +6 days. For each parameter, the time series for each year are then composited relative to the TAU times. Fig. 12 shows the mid-season composited time series of first eight of the circulation parameters defined in Table 1. The reason for us not to portray the time series of NEM3 is simply because NEM3 (17.5- 25° N, 135- 150° E), in the vicinity of Guam, shows no distinguishable signal at all. The SSM1 composite shows a period of relatively weak westerlies prior to TAU = 0, followed by a steady increase in the surface zonal wind. In addition, the notch of SSM1 clearly indicates the initiation of onset event occurs at TAU = 0, which is as expected from our definition of the onset event. Correspondingly, the same trend can be observed in the surface zonal wind over SSM2 and SSM3, except the signals are somewhat weaker. This is suggestive of a constraint on the longitudinal

extent of the change of the equatorial westerly flow, such that the mid-season event is essentially limited to the vicinity of 115° E to 135°E. From inspection of NEM1 and NEM2 , the winter monsoon winds within latitudes 17.5-25°N for the region bounded by 120-135°E and 135-150°E, respectively; the following observations can be made : 1) a higher speed prior to TAU = 0 compared to after TAU = 0 , 2) the signal of NEM2 is much stronger and persists longer than NEM1. Inspection of all other circulation parameters (NEM3, XEF1, XEF2, XEF3) indicates no significant signal, and as a result, demonstrate no apparent correspondence with the accelerated summer monsoon event.

Consequently, we turn our attention to the time series of NEM1 and NEM2 for each individual year for the same period (TAU = -5 days to TAU = +6 days) based on the time and data of TAU = 0. We see from the comparison of NEM1 for each year from 1974-1988 that the pre-onset surge of northeasterly winds is clearly delineated in seven of the fourteen years (1974, 1975, 1976, 1979, 1980, 1982, 1986), weakly delineated in three years (1981, 1985, 1987), and shows no signal at all in 1977, 1978 and in 1983. There is no mid-season event in 1984 due to missing data. For NEM2, except 1982, 1983 and 1987, the signal is much more apparent which correspondes to the result seen in the composites time series as shown in Fig 12. All of these show that an increased surface meridional wind in northern South China Sea and east of Taiwan / Philippine Islands exist prior to the southern summer monsoon onset. Once again, this suggests that there is a possible influence by the northern winter monsoon surge on the equatorial westerlies in the Indonesia-Arafura Sea region. In addition, when this influence is evident over the South China Sea, it is most pronounced in the western Pacific Ocean region east of Taiwan and the Phillippine Islands. Fig. 13 shows the composited time series of late-season area averaged parameters. As noted earlier, the late-season acceleration of the SSM1 parameter also shows a steady acceleration after TAU = 0, while SSM2 and SSM3 show no significant signal. Again, the late-season time series of SSM1, SSM2, and SSM3 show the limited longitudinal extent of the equatorial monsoonal flow. Of note, SSM1 of late-season is on average stronger than SSM1 of mid-season. The comparison of NEM1 and NEM2 indicates that NEM2 has a meridional wind peak prior to TAU = 0, the signal of NEM2 is much more obvious, and suggests that the northeasterlies strengthens for 2 or 3 days and then weakens prior to the southern summer monsoon onset. On the basis of these results we would conclude that the cold surge may influence the South Hemisphere summer monsoon onset.

Fig. 14 shows time series of WAT (surface vorticity over northwestern Australia) and SHM (Southern Hemisphere's midlatitude vorticity at the 400 mb level over

Southwestern Australia) for both mid-season and late-season. For mid-season , there is no significant correlation in between WAT and SSM1 ,as well as between SHM and SSM1. On the other hand, in the late-season event the SHM parameter is well correlated with the SSM1 parameter in this case. There is a significant increase in SHM three days prior to TAU = 0 and a steady decrease after TAU = 0 as shown in Fig. 14(b). This may be related to the results pointed out by Davidson et al.(1983). Their observations reveals that, prior to onset, the major baroclinic development in the South Hemisphere midlatitude upper level takes place and is a possible forcing mechanism triggering the monsoonal convection north of Australia. Although the events referred to by Davidson et al. (1983) usually occur in late December versus the late-season events identified in this study. There is also an increase in WAT 2 to 3 days prior to the onset. This signal is not as strong as the SHM parameter. Nevertheless, both studies suggest a possible role of the Southern Hemisphere midlatitude baroclinic system in influencing tropical monsoonal circulation. It is probable that these midlatitude activities trigger the surges west of Australia in a manner similar to the northern winter cold surges.

B. COMPOSITE MAP SEQUENCE

To obtain a two-dimensional perspective of the relationship between the northeast monsoon surge and the downstream flow changes in the equatorial region and the Southern Hemisphere, maps of surface horizontal wind are composited according to the development of the mid-seasons events. Fig. 15 shows the composite maps at 24 hours intervals from TAU = -120 hours (TAU = -5 days) to TAU = + 144 hours (TAU = + 6 days). The reason of using 24-hour intervals is to remove the influence of diurnal effects. Fig. 15 indicates that the northeasterly monsoonal winds at TAU = -72 hours reach its maximum prior to a mid-season event. The strongest northeast winds are concentrated in the South China Sea extending from north of Taiwan southwestward towards the Malay Penisula and Sumatra. This is in the same area as the maximum mean northeast winds indicated in the 14-year mean (Fig. 1). Outside of the South China Sea the northeasterlies spread over a very broad longitudinal domain that covers almost the entire tropical North Pacific, but the latitudinal extent is mostly confined to 5^0 N- 20^0 N. After TAU = 0, the surface northeasterlies gradually decreases, and although the regime of 10 ms^{-1} isotach becomes much smaller, a region of maximum wind (> 10 ms^{-1}) persists in the South China Sea throughout the period.

Correspondingly, the zonal wind along 10^0 S in the Indonesia-Arafura Sea region is westerly but weak and of little extent before TAU = 0. After TAU = 0, the westerlies

strengthen and expand eastward from about 120° E. The western Australian surface low persists throughout the period. The southerly wind surge along the western Australian coast shows an enhancement from TAU = + 72 hours on. It is worthwhile to note that a regime of southeastly winds present off the northeast of Australia, and increse in strength at TAU = -24 hours.

The above observation depicts that the northeasterly winds strengthen prior to summer monsoon onset for the mid-season events. So, the results support Lim and Chang's(1981) hypothesis which emphasizes the winter monsoon cold surge may have such a cross-equatorial influence on Southern Hemisphere's summer monsoon. (The maps for the late season events are not composited because the signals of correlated upstream motion are less clear.)

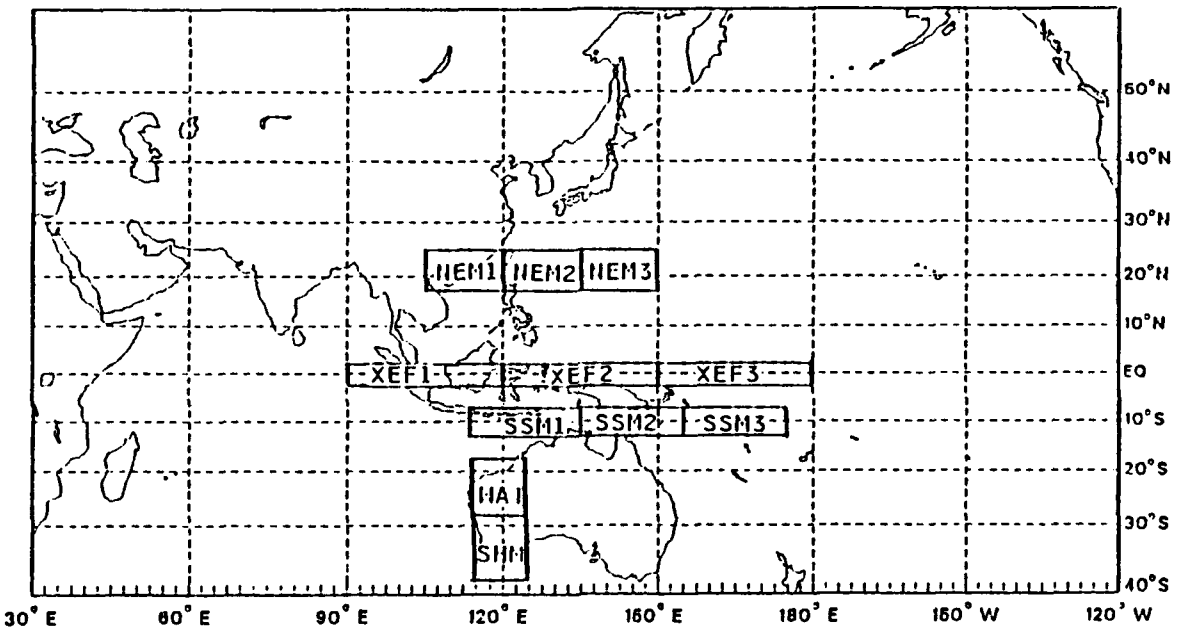

Fig. 10. Map showing different areas over which the parameters indicated are averaged.

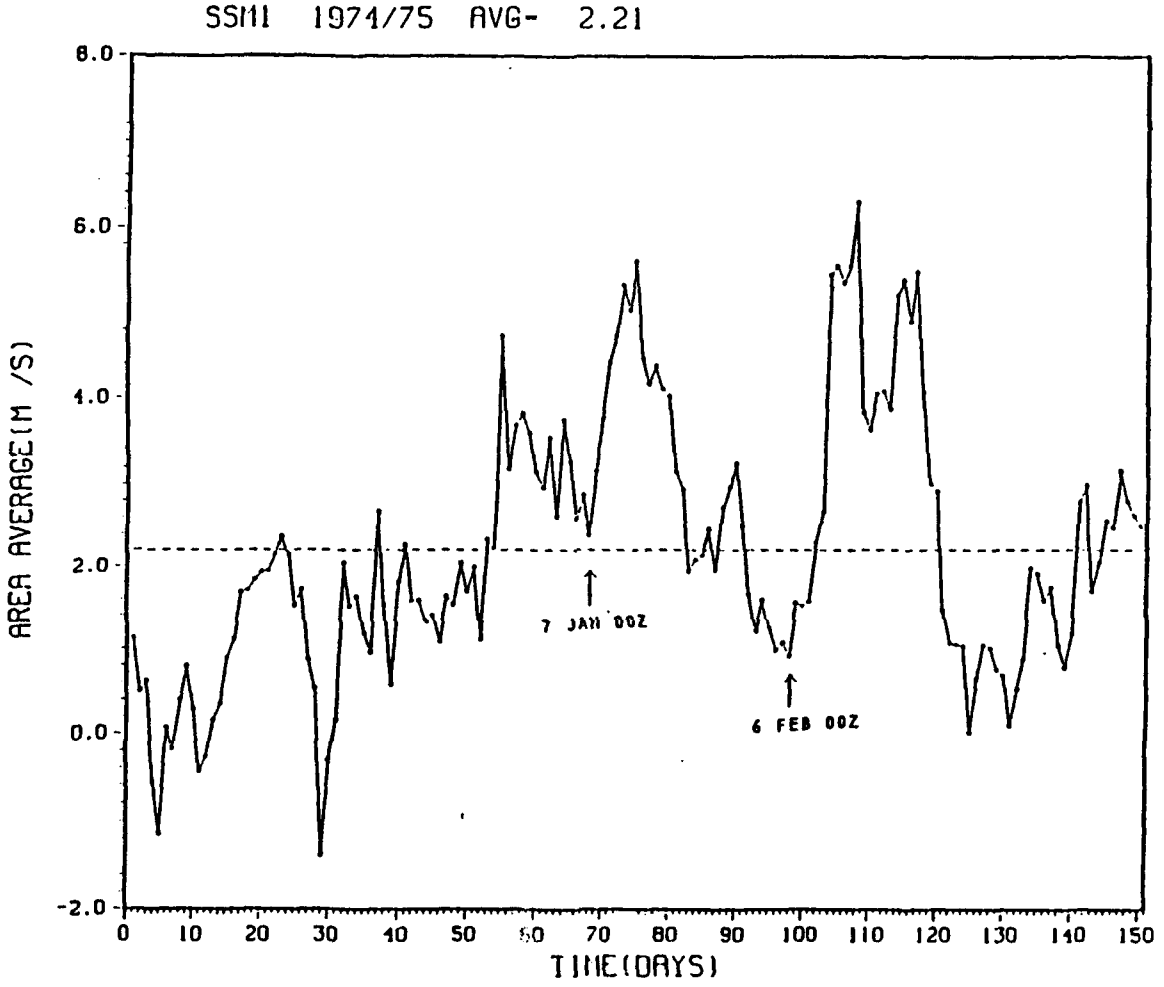

Fig. 11. Time series of area-averaged surface zonal wind over the Indonesia-Arafura Sea region.

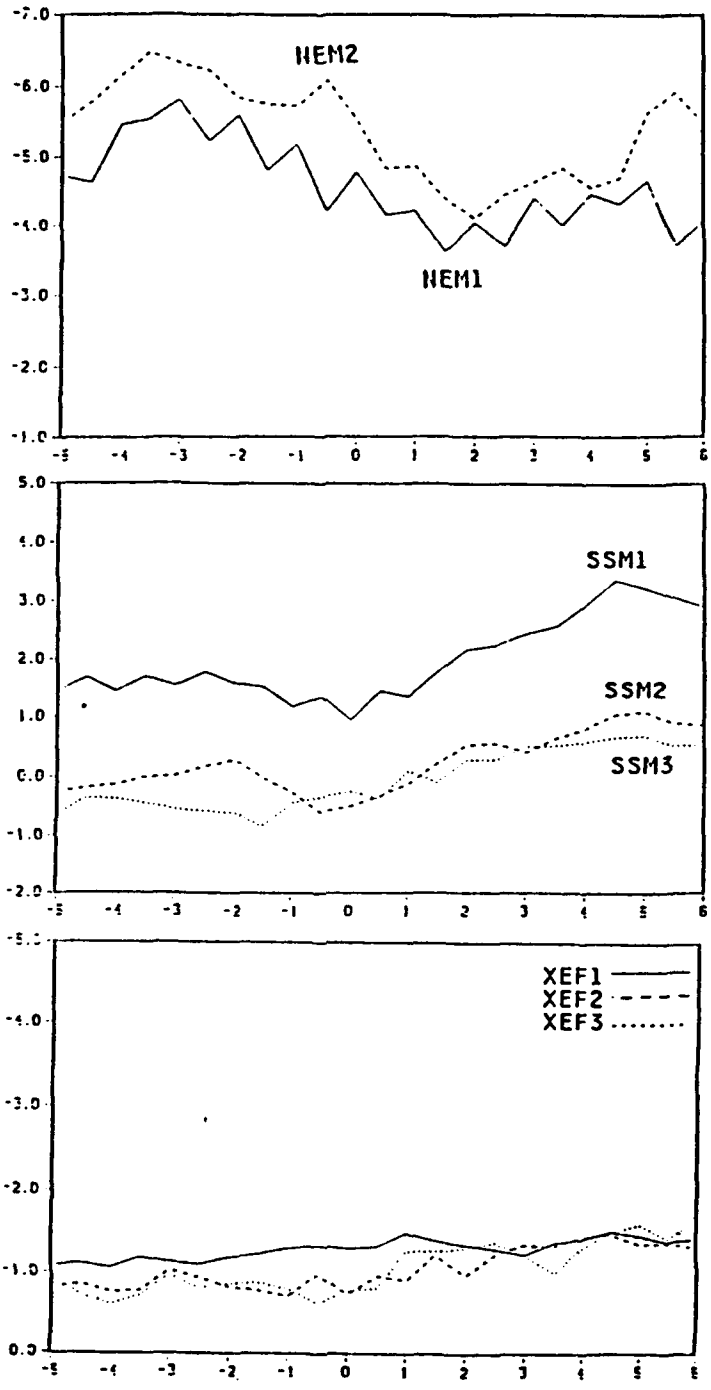

Fig. 12. Time series of mid-season composited area averaged parameters. The abscissa is the period from tau = -5 days to tau = + 6 days. The ordinate is the wind speed in ms^{-1}.

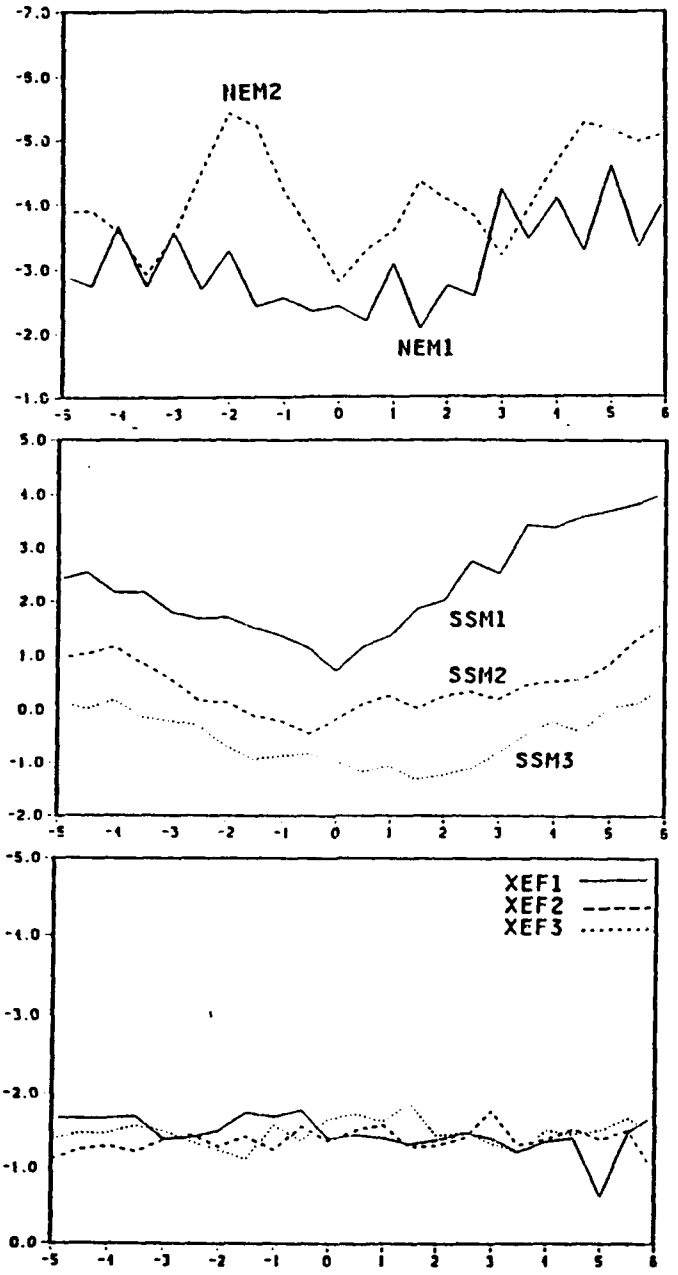

Fig. 13. Time series of late-season composited area averaged parameters. The abscissa is the period from tau = -5 days to tau = + 6 days. The ordinate is the wind speed in ms^{-1}.

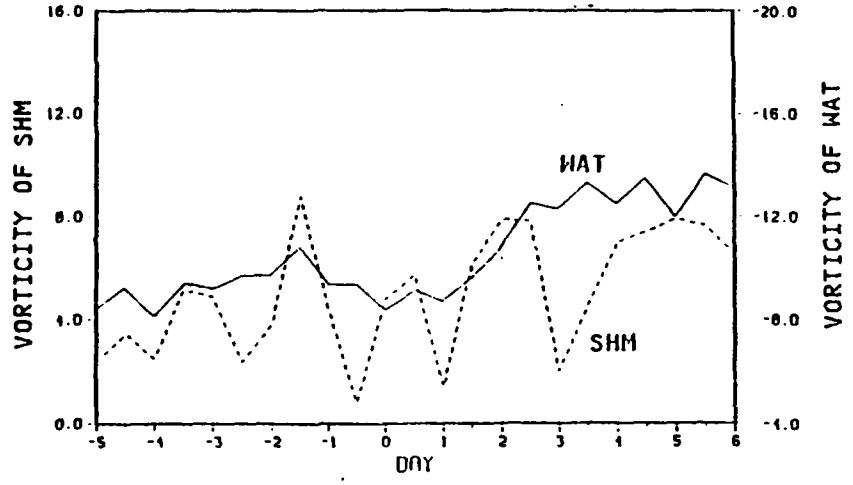

(a)Mid-season

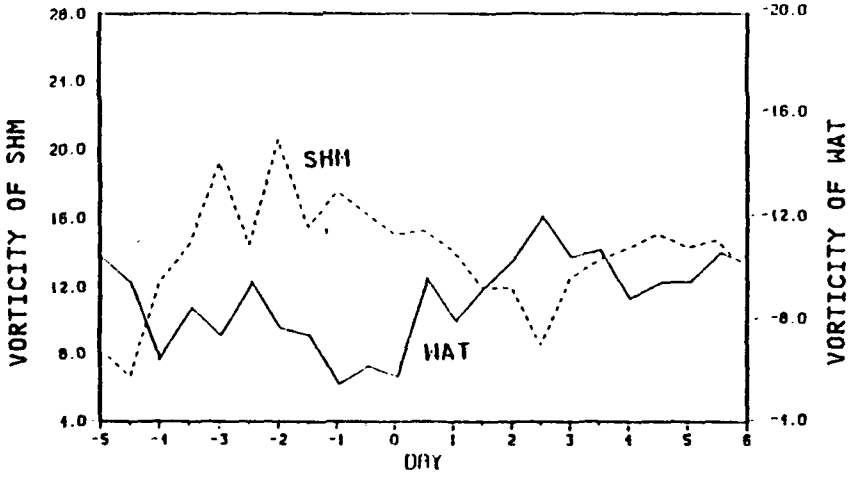

(b)Late-season

Fig. 14. Time series of composited area averaged parameters for WAT and SHM.(a)mid-season event.(b)late-season event. The ordinate is vorticity in $10^{-6}s^{-1}$.

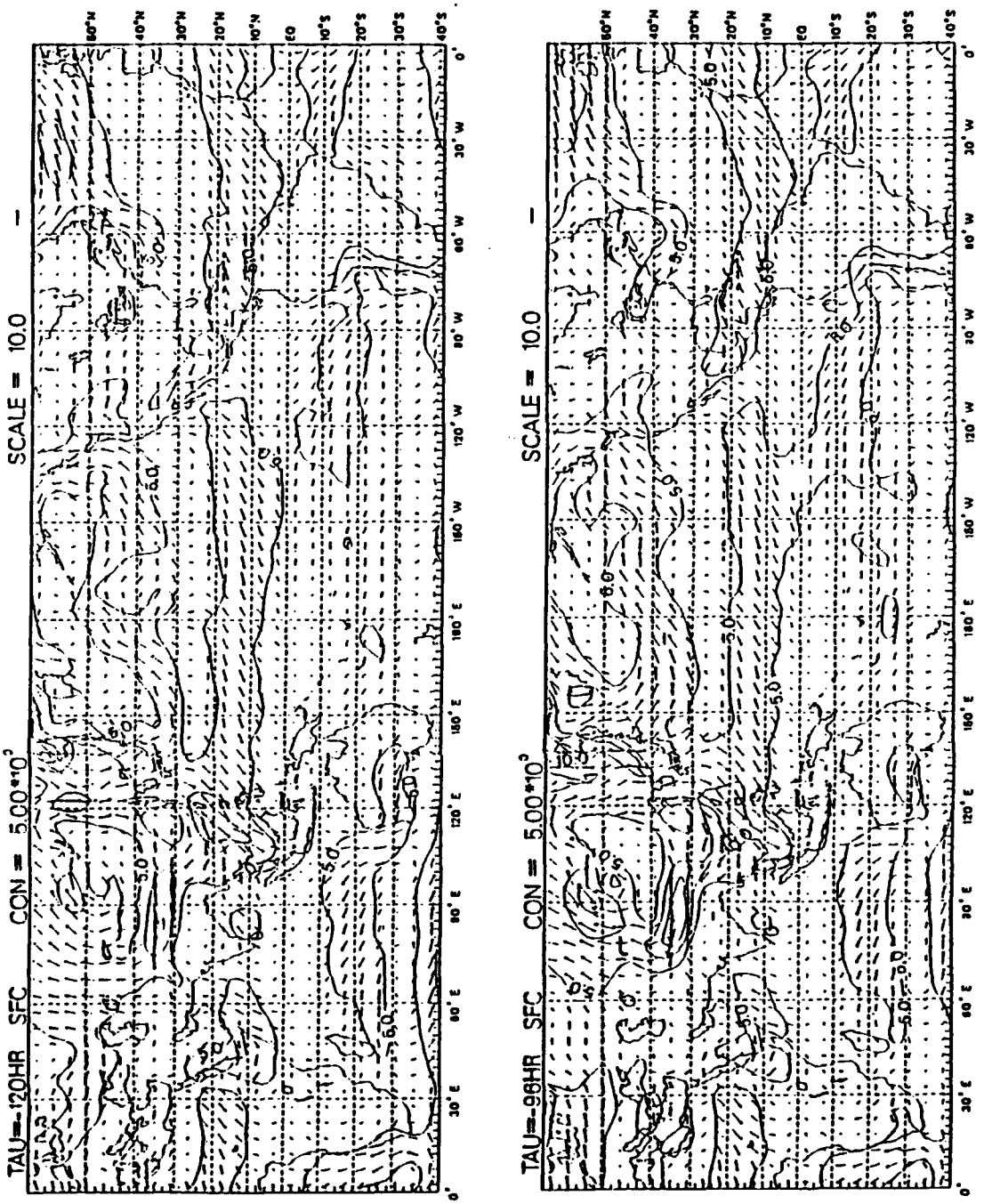

Fig. 15. Composite maps of surface horizontal wind at 24-hour time interval.

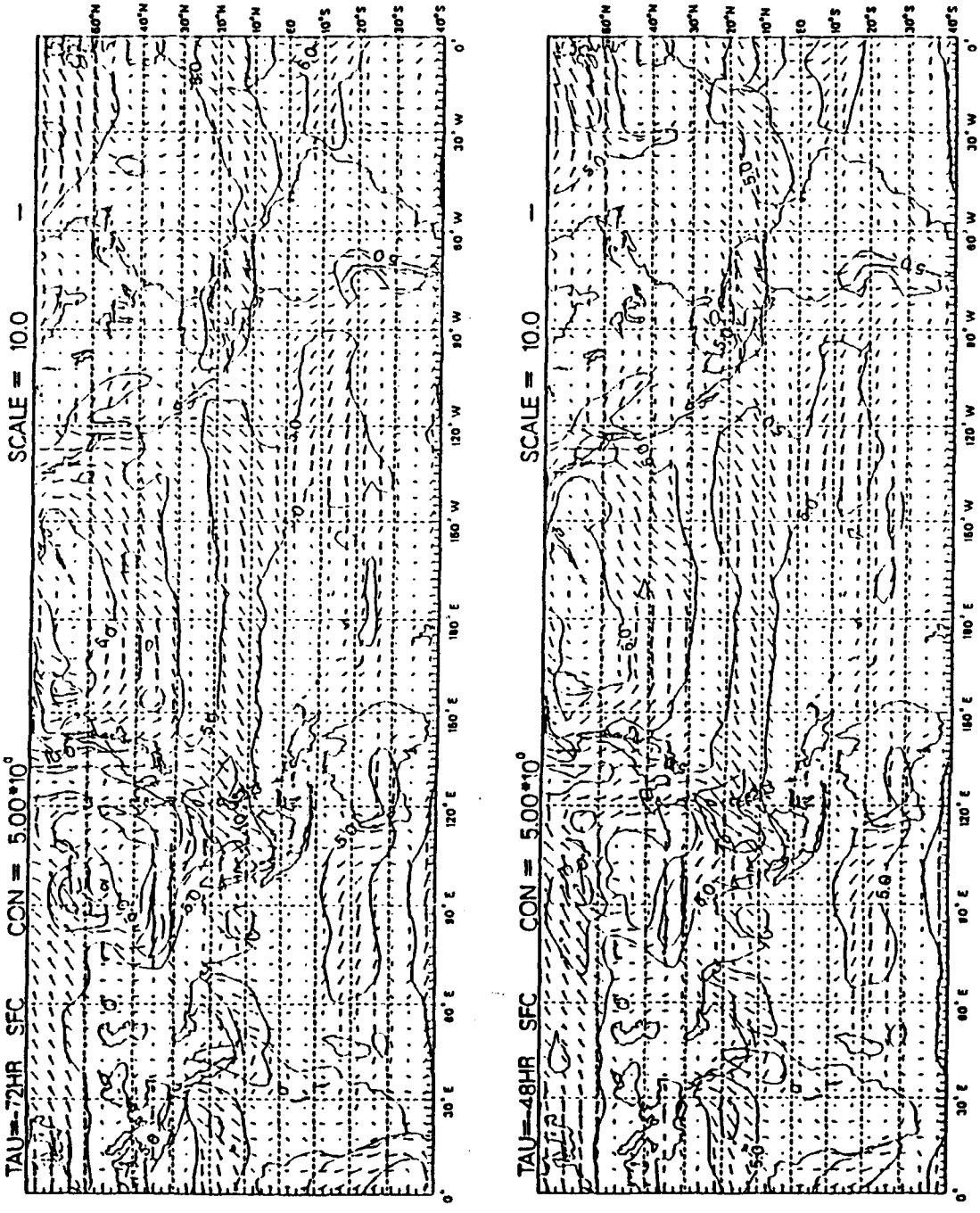

Fig. 15. (Continued)

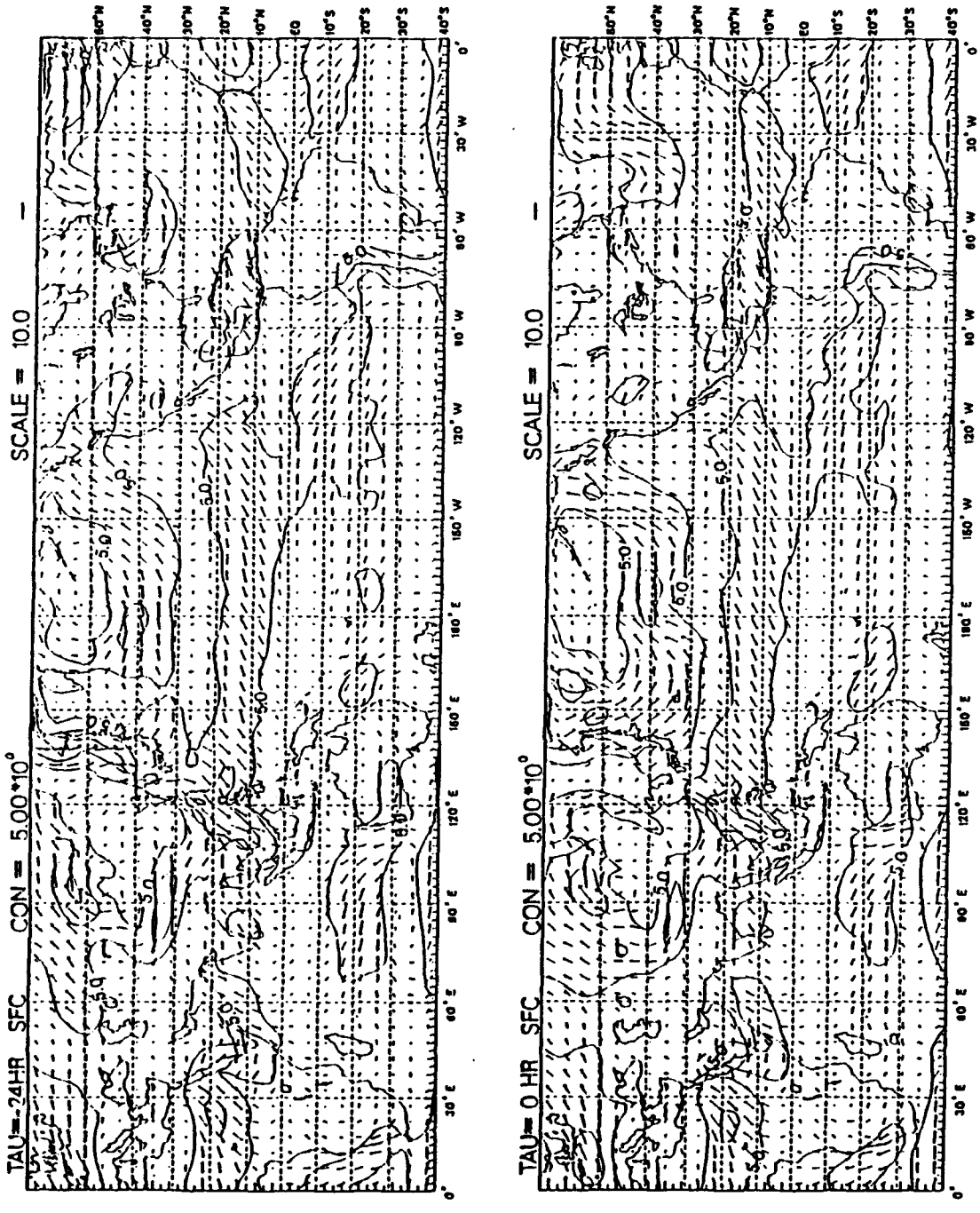

Fig. 15. (Continued)

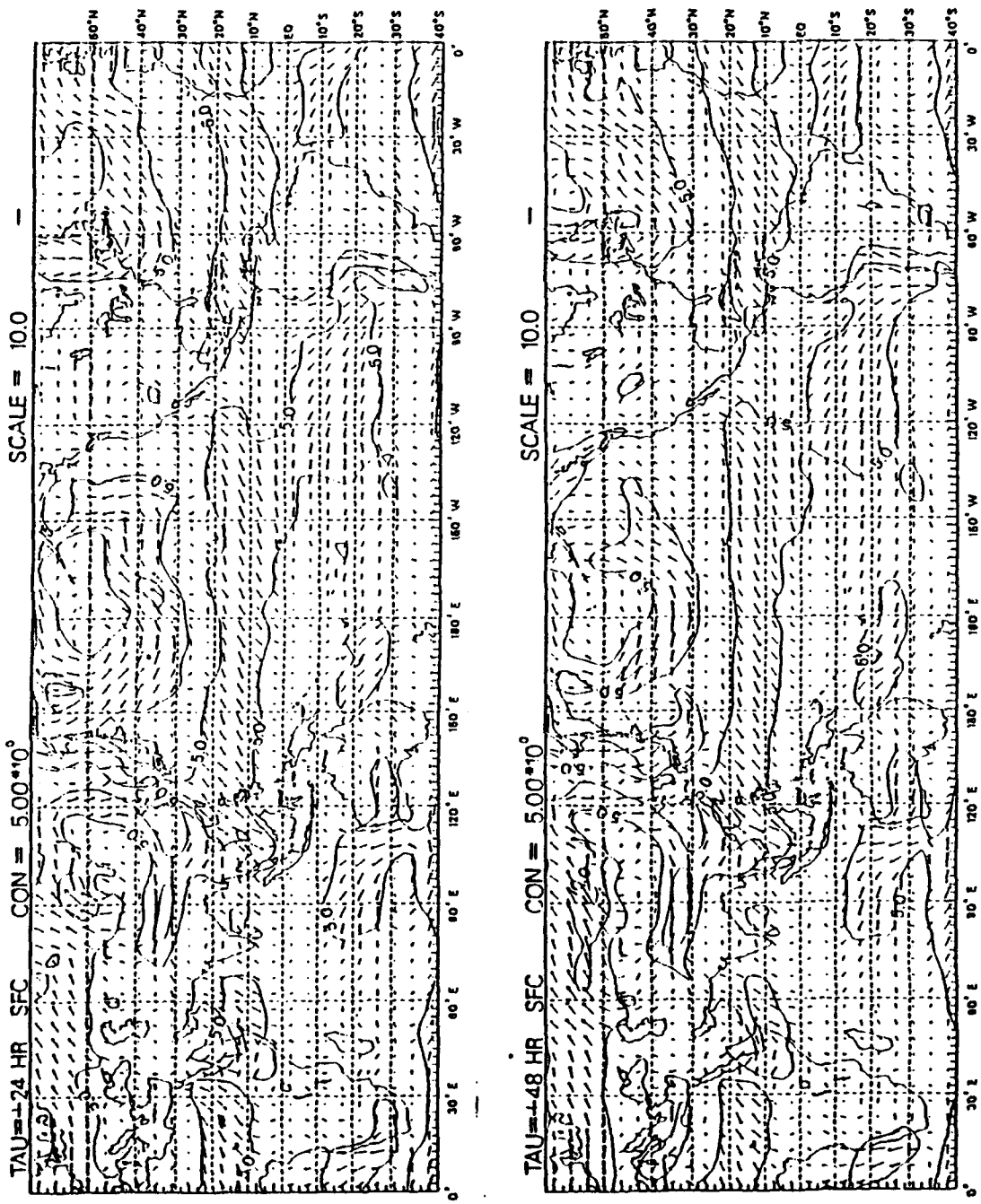

Fig. 15. (Continued)

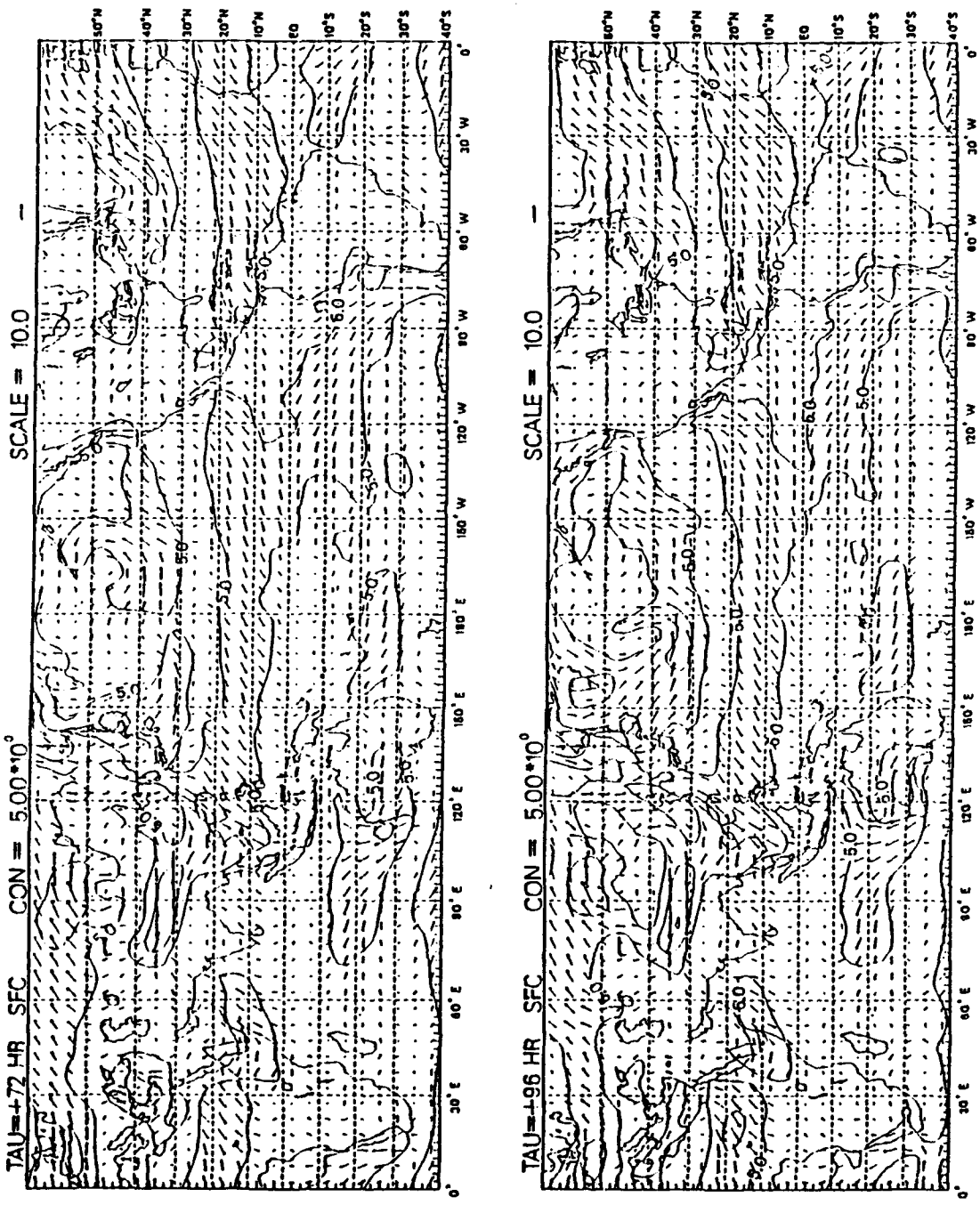

Fig. 15. (Continued)

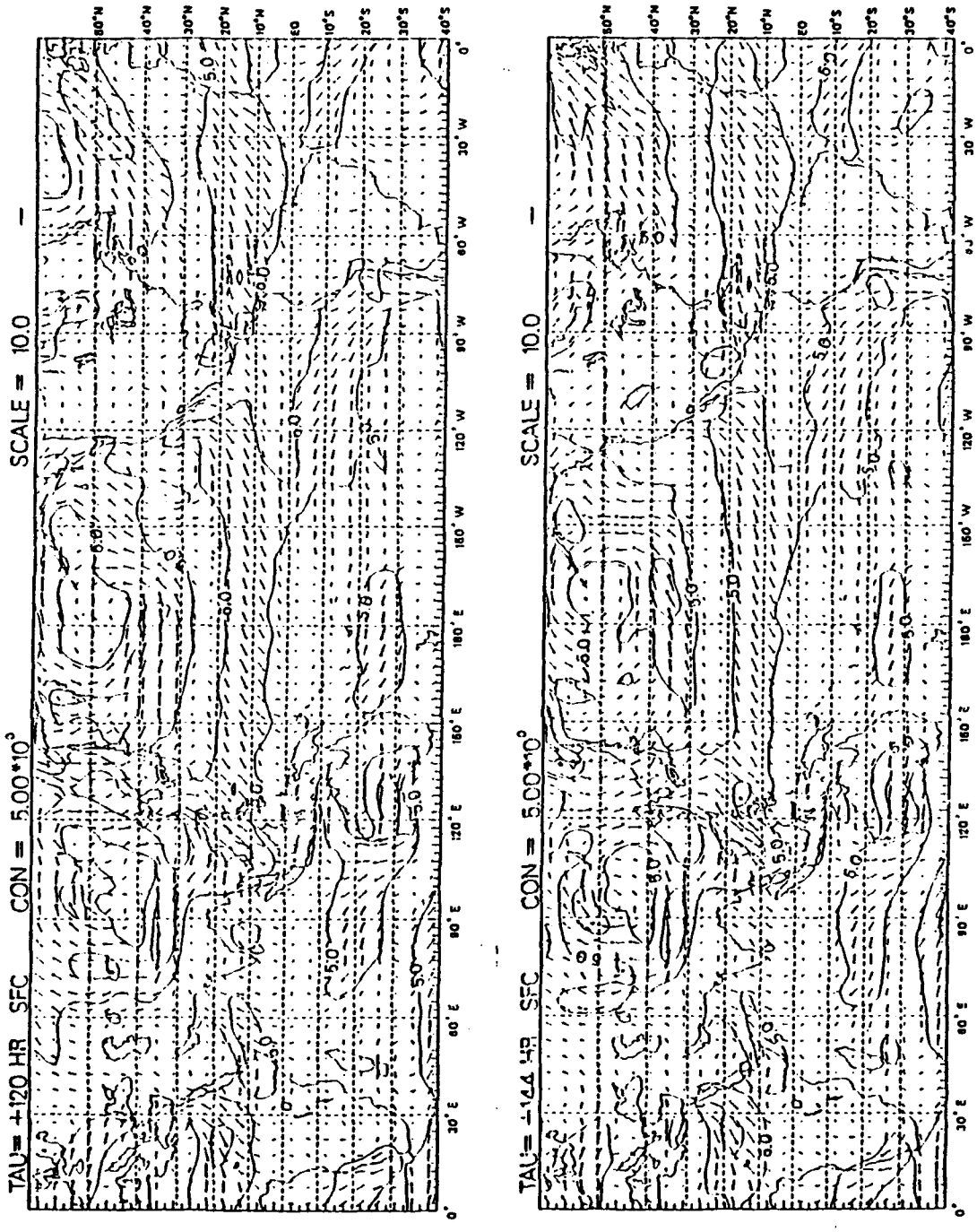

Fig. 15. (Continued)

Table 1. AREA AVERAGED PARAMETERS

Parameter	Data and area	Circulation components represented
NEM1	Surface meridional wind in northern South China Sea (17.5 - 25°N, 105 -120°E)	Winter monsoon surge
NEM2	Surface meridional wind east of Taiwan / Philippine Islands (17.5 -25°N , 120 - 135°E)	Winter monsoon surge
NEM3	Surface meridional wind over Guam and vicinity (17.5 -25° N,135 -150°E)	Winter monsoon surge
XEF1	Surface meridional wind over maritime continent(2.5°S- 2.5° N , 90-120°E)	Cross equatorial flow
XEF2	Surface meridional wind north of New Guinea (2.5°S- 2.5° N ,120 -150°E)	Cross equatorial flow
XEF3	Surface meridional wind over equatorial Pacific Ocean(2.5° S - 2.5°N ,150°E -180°)	Cross equatorial flow
SSM1	Surface zonal wind over Indonesia-Arafura Sea region(12.5- 7.5° S ,115 - 135°E)	Equatorial monsoonal flow
SSM2	Surface zonal wind over Southern New Guinea (12.5- 7.5°S , 135 -155°E)	Equatorial monsoonal flow
SSM3	Surface zonal wind over Honiara and vicinity (12.5 -7.5°S , 155 -175°E)	Equatorial monsoonal flow
WAT	Surface vorticity over Northwestern Australia (27.5-17.5° S, 115-125°E)	Surface heat low
SHM	400 mb vorticity over southwestern Australia (37.5 - 27.5°S , 115 - 125°E)	Midlatitude mid-troposphere effect

NEM = Northeast Monsoon

XEF = Cross-equatorial Flow

SSM = Southern Summer Monsoon

WAT = Western Australia Trough

SHM = Southern Hemisphere Monsoon

Table 2. SUMMARY OF DATE/TIME OF TAU=0 FOR MID- AND LATE-SEASON COMPOSITING OF AREA

Season	Date and Time (Mid-season)	Date and Time (Late-season)
1974-1975	07 Jan / 00GMT	06 Feb / 00GMT
1975-1976	31 Dec / 00GMT	30 Jan / 00GMT
1976-1977	31 Dec / 12GMT	29 Jan / 00GMT
1977-1978	31 Dec / 00GMT	13 Jan / 12GMT
1978-1979	21 Dec / 12GMT	
1979-1980	28 Dec / 00GMT	23 Jan / 00GMT
1980-1981	30 Dec / 00GMT	
1981-1982	08 Jan / 00GMT	
1982-1983	28 Dec / 00GMT	
1983-1984	04 Jan / 00GMT	03 Feb / 00GMT
1984-1985		15 Feb / 00GMT
1985-1986	15 Jan / 00GMT	
1986-1987		27 Jan / 00GMT
1987-1988	18 Dec / 00GMT	05 Feb / 00GMT

V. SUMMARY AND CONCLUSIONS

The purpose of this research was to extend Shield's (1985) study on the possible influences of the northeast monsoon in the Northern Hemisphere on the Southern Hemisphere's summer monsoon by using a 14-year data set. The data used were from the operational Global Band Analysis of the Fleet Numerical Oceanography Center and covered the nothern winter seasons of 1974-75 through 1987-88. The main level of study was the surface, where the Global Band Analysis's surface marine wind field was based on a wealth of island station and ship wind reports in the area of study.

Time-mean circulation charts of wind, velocity potential and streamfunction were compiled. These charts allowed the identification of major tropical low-level circulations during the northern winter. Among them, the surface northeast monsoonal winds in the South and East China Seas region, and the western Australian trough were the most noticeable features.

The time evolutions of the circulation features were studied using a composite method. The strengthening of the southern equatorial surface westerlies along 10^0 S in the Indonesia-Arafura Sea region was considered a manifestation of the development of active southern summer monsoon, and was used as the base series in the compositing. For each of the seasons the development of significant acceleration of the westerlies was identified, and the timing of these developments was used as the base reference for compositing other circulation parameters. In most of the seasons the major developments occur around either late December-early January, and or in February. Events occurred in the former period were called the mid-season events, and those occurred in the latter period were called the late-season events. The composite of the time series of the various variables were done separately for the two types of events.

The major circulation features were each represented by one or more area-averaged variables. The northeasterly surge in the northern subtropics was represented by the surface meridional wind averaged over three sections across from the South China Sea to the western Pacific. The cross-equatorial flow was also represented by the surface meridional wind averaged over three sections along the equator. The surface westerlies along 10^0 S was represented by surface zonal winds, and also averaged in three sections. Two Southern Hemispheric circulation systems were included: the western Australian

surface trough, and the upper tropospheric midlatitude baroclinic waves. They were represented by area-averaged vorticity at surface and 400 mb, respectively.

The following conclusions are based on an examination of the composited area averaged time series parameters and the composite surface wind analysis:

1) Prior to the onset of the mid-season event of the westerly acceleration in the southern tropics, the northeasterlies in the South China Sea (NEM1) and in the vicinity of Taiwan and Philippine Islands (NEM2) show a general tendency of increasing wind speed. The characteristic of the northeasterly surge in the vicinity of Taiwan and Philippine Islands is stronger and persists longer than that in the South China Sea. Immediately after the onset of mid-season event, the northeasterlies in the Taiwan and Philippines vicinity also decelerate more rapidly.

2) For the late-season event of the southern tropics zonal wind acceleration, there is no significant signal associated with the change in the northeasterlies in the South China Sea. However, the northeasterly surge in the vicinity of Taiwan and Philippine Islands is strengthened dramatically about two days prior to the southern onset, and then rapidly decelerated.

3) During the mid-season event, the zonal wind acceleration is concentrated in Indonesia-Arafura Sea region (SSM1 and SSM2) , while in the late-season event the zonal wind acceleration is limited primarily in the western part of this region (SSM1) only. This implies that westerly monsoonal flow acceleration along 10^0 S is longitudinally limited.

4) For late-season events, the most pro[illegible]nced circulation feature that was correlated to the development of westerly accelerations in the southern tropics is the 400 mb midlatitude westerlies (SHM). It enhanced immediately prior to the onset. The vorticity of the western Australian trough (WAT) also enhanced prior to the late-season onset. These correlations suggest that a surge of southerly wind parallel to the West Australian coastline and anticyclogenesis over southwestern and south-central Australia are related to the westerly acceleration.

5) All the other circulation features, including the northeasterly monsoon winds in the western Pacific (NEM3), and the cross-equatorial flows along the equator (XEF1, XEF2, and XEF3), displayed no significant correlation with the development of the southern summer monsoon. This indicates that cross-equatorial flow may not be a good indicator of the effects of the Northern Hemisphere monsoonal wind on the Southern Hemisphere summer monsoonal flow.

Because of the different features of mid-season event and late-season event, we suggest that mid-season events in the southern summer monsoon is influenced by surges in the northeast monsoon in the Northern Hemisphere, while the late-season events in the southern summer monsoon may be due entirely to midlatitude baroclinic development rather than the cold surges from the Northern Hemisphere. However, the cause-effect relationship of the observed interactions remain somewhat unclear. Some of the observational works reviewed in the introduction have different results, including suggestions that the northern winter monsoon surges should affect the Southern Hemisphere throughout the seasons, or that the southern summer monsoon is entirely a Southern Hemisphere phenomena independent of the nortern winter monsoon. These different results may be partly due to the complexity of the monsoons. Different forcing mechanisms (e.g., South China Sea surges, West Australian surges) may come into play under different circumstances, and sometime it may not be easy to separately identify their respective effects. The work conducted here was limited to the surface wind composites. Further observational and theoretical studies are necessary to understand the interactions between Southern Hemisphere monsoon and the Northern Hemisphere monsoon systems.

REFERENCES

1. Berson, F.A., 1961: Circulation and energy balance in a tropical monsoon. *Tellus, 13*, 472-485.

2. Berson, F.A., and A.J. Troup, 1961: On the angular momentum balance in the equatorial trough zone of the eastern hemisphere. *Tellus, 13*, 66-78.

3. Bjerknes, J., 1969: Atmospheric teleconnections from the equatorial Pacific. *Mon. wea. Rev., 97*, 163-172.

4. Boyle, J.S., and K.-M. Lau, 1984: Monthly seasonal climatology over the global tropics and subtropics for the decade 1974 to 1983. Volume II: Outgoinglongwave radiation. NPS Technical Report NPS-63-84-007. Naval Postgraduade School, Monterey, Ca, 58pp.

5. Chang, C.-P., J. E. Erickson and K. M. Lau, 1979: Northeasterly cold surges and near-equatorial disturbances over the Winter MONEX area during December 1974. Part I: Synoptic Aspects. *Mon. Wea. Rev. 107*, 812-829.

6. Chang, C.-P., and K.-M. Lau, 1980: Northeasterly cold surges and near-equatorial disturbances over the winter MONEX area during December 1974. Part II: Planetary-scale aspects. *Mon. Wea. Rev., 108*, 298-312.

7. Cressman, G.P., 1959: An operational objective analysis system. *Mon. Wea. Rev., 87*, 367-374.

8. Davidson, N.E., J.L. McBride and B.J. McAvaney, 1983: The onset of the Australian Monsoon during winter MONEX: synoptic aspects. *Mon. Wea. Rev., 111*, 496-516.

9. Davidson, N.E., 1984: Short term fluctuations in the Australian Monsoon during winter MONEX. *Mon. Wea. Rev. 112*, 1697-1708.

10. Gray, W. M., 1968: Global view of the origin of tropical disturbances and storms. *Mon. Wea. Rev. 96*, 669-700.

11. Holland, G.T., T.D. Keenan and A.E. Guymer, 1984: The Australian monsoon: Definition and variability. Postprint volume, 15th Conference on Hurricanes and Tropical Meteorology, Miami, Fl., January 1984. American Meteor. Soc., Boston, Ma., P. 398-402.

12. Holland, G. T., and N. Nicholls, 1985: A simple predictor of EL Niño? *Trop. Ocean-Atmos. Newslett. 30*, 8-9.

13. Johnson, R.H., 1982: Vertical motion in near-equatorial winter MONEX convection. *J. Meteor. Soc. Japan, 60*, 682-690.

14. Krishnamurti, T. N., N. Kanamistsu, W. J. Koss and J. d. Lee, 1973: Tropical east-west circulations during the northern winter. *J. Atmos. Sci. 30*, 780-787.

15. Lewis, J.M., and T.H. Grayson, 1972: The adjustment of surface wind and pressure by Sasaki's variational matching technique. *J. Appl. Meteor., 11*, 586-597.

16. Lim, H.,and C.-P. Chang, 1981: A theory of midlatitude forcing of tropical motions during winter monsoon. *J. Atmos. Sci., 38*, 2377-2392.

17. McBride, J. L.,1983b: Australian tropical weather systems. In *Extended abstracts, Australian conference on tropical meteorology, Melbourne, March 24-25, 1983.* Bureau of Meteorology, Melbourne.

18. Murakami, T.,and A. Sumi, 1982a: Southern hemisphere summer monsoon circulation during the 1978-79 WMONEX. part I: Monthly mean wind fields. *J. Meteor. Soc. Japan, 60*, 638-648.

19. Murakami, T.,and A. Sumi, 1982b: Southern hemisphere summer monsoon circulation during the 1978-79 WMONEX. part II: Onset, active and break monsoons. *J. Meteor. Soc. Japan, 60*, 649- 671.

20. Oort, A.H., 1983: Global atmospheric circulation statistics, 1958- 1973. NOAA Professional Paper 14. U.S. Department of Commerce (available from the Superintendent,Washington, D.C. 20402).

21. Ramage, C.S., 1971: *Monsoon Meteorology*, Academic Press, 296 p.

22. Shield, K. A., 1985: Possible cross equatorial influence of the northeast monsoon on the equatorial westerlies over Indonesia. NPS Thesis. Naval Postgraduate School, Monterey, Ca, 73pp.

23. Shukla, J.,and K.R. Saha, 1974: Computation of non-divergent streamfunction and irrotational velocity potential from observed winds. *Mon. Wea. Rev., 102*, 419-425.

24. Sumi, A , and T. Murakami, 1981: Large scale aspects of the 1978-79 winter circulation over the greater WMONEX region. Part I: Monthly and season mean fields. *J. Meteor. Soc. Jpn. 59*, 625-645.

25. Troup, A.J., 1961: Variation in upper tropospheric flow associated with the onset of the Australian summer monsoon. *Indian J. Meteor. Geophys., 12*, 217-230.

INITIAL DISTRIBUTION LIST

		No. Copies
1.	Defense Technical Information Center Cameron Station Alexandria, VA 22304-6145	2
2.	Library, Code 0142 Naval Postgraduate School Monterey, CA 93943-5002	2
3.	Chairman (Code 63Rd) Department of Meteorology Naval Postgraduate School Monterey, CA 93943-5000	1
4.	Professor C.-P. Chang (Code 63CP) Department of Meteorology Naval Postgraduate School Monterey, CA 93943-5000	1
5.	Professor M.S. Peng (Code 63PG) Department of Meteorology Naval Postgraduate School Monterey, CA 93943-5000	1
6.	LCDR Chen, Chih-lyeu smc#1275 NPS Monterey, CA 93943	2
7.	Director Naval Oceanography Division Naval Observatory 34th and Massachusetts Avenue NW Washington, DC 20390	1
8.	Commander Naval Oceanography Command Stennis Space Center, MS 39529-5000	1
9.	Commanding Officer Naval Oceanographic Office Stennis Space Center, MS 39522-5001	1
10.	Commanding Officer Fleet Numerical Oceanography Center Monterey, CA 93943	1
11.	Commanding Officer Naval Ocean Research and Development Activity Stennis Space Center, MS 39522-5001	1

12. Director
Naval Oceanographic and Atmospheric Laboratory
(Monterey Detachment)
Monterey, CA 93943 — 1

13. Naval Weather Center
P.O. Box 90158, PA-LI, Taipei county
Taiwan, R.O.C. — 2

14. Chief of Naval Research
800 North Quincy Street
Arlington, VA 22217 — 1

15. Office of Naval Research (Code 420)
Naval Ocean Research and Development Activity
800 North Quincy Street
Arlington, VA 22217 — 1

16. LCDR Chen, chih-lyeu
4F, 10, Lane 70, Yu-Feng Street, Ku-hsan
Kaohsiung, Taiwan, R.O.C. — 3

17. Scientific Liaison Office
Office of Naval Research
Scripps Institution of Oceanography
La Jolla, CA 92037 — 1